A simulation approach to the thermal-hydraulic design of cored ceramic brick regenerative heat exchangers

by Gary Alan Upshaw

A thesis submitted in partial fulfillment of the requirements for the degree of MASTER OF SCIENCE in Mechanical Engineering
Montana State University

Abstract:
Using the cored brick regenerative heat exchanger as a basis, a method for designing heat exchangers to supply preheated air for open cycle magnetohydrodynamic power generation systems was developed.

Design information and significant performance trends for multiple unit MHD air preheater systems were explored using a digital computer model which simulated operation of a cored brick regenerative heat exchanger. Thermal-hydraulic designs using numerous variations of core geometry and cycling parameters were completed to meet flow and temperature specifications of a typical full scale air preheater system. Unique values for flow rates, heat exchanger core sizing and ceramic mass requirements were calculated for each of these variations using criteria of limited thermally induced stress in the ceramic,specific discharge temperature for the preheated air stream and limited blowdown exit temperature droop.

Simulations using variations in tube roughness show minimal difference in total ceramic mass requirements. The model was used to determine the sensitivity of an air preheater performance to variation in flow and geometric parameters. Thermal operational characteristics of a cored brick heat exchanger test facility are predicted for several variations in flow rates and total cycle times.

STATEMENT OF PERMISSION TO COPY

In presenting this thesis in partial fulfillment of the requirements for an advanced degree at Montana State University, I agree that the Library shall make it freely available for inspection. I further agree that permission for extensive copying of this thesis for scholarly purposes may be granted by my major professor, or, in his absence, by the Director of Libraries. It is understood that any copying or publication of this thesis for financial gain shall not be allowed without my written permission.

Signature Gary A. Upshaw

Date 5/17/77

A SIMULATION APPROACH TO THE THERMAL-HYDRAULIC DESIGN OF CORED CERAMIC BRICK REGENERATIVE HEAT EXCHANGERS

by

GARY ALAN UPSHAW

A thesis submitted in partial fulfillment
of the requirements for the degree

of

MASTER OF SCIENCE

in

Mechanical Engineering

Approved:

Thomas G Berhman
Chairperson, Graduate Committee

D.O. Bhekketter by RC Challender
Head, Major Department

Henry L Parsons
Graduate Dean

MONTANA STATE UNIVERSITY
Bozeman, Montana

June, 1977

ACKNOWLEDGEMENTS

The author acknowledges and thanks Dr. T. C. Reihman and Dr. H. W. Townes for their guidance and assistance in the preparation and completion of this thesis.

The author would like to thank his family and friends for their support and encouragement. Finally, I thank my wife, Janet, for her untiring support and patience through the entirety of this research and for her typing of this thesis.

TABLE OF CONTENTS

LIST OF TABLES

LIST OF FIGURES

Nomenclature

a	=	inner radius of tube	[m]
A1	=	flow area	[m^2]
A2	=	area enclosed by adiabatic surface	[m^2]
BTI	=	blowdown time	[sec]
b	=	equivalent outside tube radius	[m]
C_p	=	specific heat	[$J/_{kg}$-K]
D	=	hole diameter	[m]
D2	=	equivalent outside tube diameter	[m]
E	=	modulus of elasticity of ceramic	[Pa]
f	=	Darcy-Weisbach friction factor	
h	=	convective heat transfer coefficient between gas and ceramic surface	[W/m^2-K]
h.x.	=	heat exchanger (abbreviation)	
k	=	thermal conductivity	[W/m-K]
K_s	=	tube roughness	[m]
L	=	bed length	[m]
ln	=	logarithm to base e	
$\dot{m}$	=	mass flow rate	[kg/sec]
NB	=	number of heat exchangers in blowdown mode	
NR	=	number of heat exchangers in reheat mode	
Nu	=	local Nussult number (hD/k_g)	

Nomenclature

P1	=	inlet reheat gas pressure	[Pa]
P2	=	inlet blowdown air pressure	[Pa]
Pr	=	Prandtl number ($C_{pg}\ \mu_g/k_g$)	
Q	=	heat flux between gas and ceramic	[W/m^2]
R	=	gas constant	[J/kg-K]
Re	=	Reynolds number ($\mu_g V_g D/\mu_g$)	
RTI	=	reheat time	[sec]
S	=	hole to hole spacing	[m]
S/D	=	ratio of hole spacing to hole diameter	[m/m]
STI	=	switchover time	[sec]
T	=	temperature	[K]
T(J,I)	=	temperature of ceramic in lumped mass model at axial location J and time I. Time I=1 is present time, t, and time I=2 is time at t+Δt	[K]
TEXIT	=	average exit gas temperature	[K]
TG(J)	=	gas temperature in lumped mass model at axial position J	[K]
TGI1	=	inlet reheat gas temperature	[K]
TGI2	=	inlet blowdown air temperature	[K]
t	=	time	[sec]
Δt	=	time increment	[sec]
V	=	local mean gas velocity	[m/sec]

Nomenclature

$V1$ = inlet reheat gas velocity [m/sec]

$V2$ = inlet blowdown air velocity [m/sec]

X = axial distance along tube [m]

Z = axial direction coordinate

ΔZ = length increment in axial direction [m]

α = thermal diffusivity $(k_c/\rho_c C_{pc})$

$$\alpha_1 = \frac{2\ h\ a\ \Delta t}{\rho_c C_{pc}(b^2-a^2)}$$

$$\alpha_2 = \frac{2\ h\ a\ \Delta Z}{\dot{m}\ C_{pg}}$$

$$\alpha_3 = \frac{k\ \Delta t}{\rho_c C_{pc}\ \Delta Z^2}$$

$$\alpha_6 = \frac{h\ a\ b^2}{k_c(b^2-a^2)}\left[\frac{a^2}{2b^2} - \frac{b^2+a^2}{4b^2} + \frac{b^2}{b^2-a^2}\ln\left(\frac{b}{a}\right) - \frac{1}{2}\right]$$

β = thermal coefficient of expansion for ceramic [m/m-K]

μ = dynamic viscosity [Pa-sec]

ν = Poisson's ratio for ceramic

ρ = density [kg/m^3]

σ = thermal stress [Pa]

Δ = increment designation

Subscripts

a = inner wall

avg = average

BD = blowdown

C = ceramic

conv = convection

g = gas

0 = smooth pipe

RH = reheat

r = rough pipe

ABSTRACT

Using the cored brick regenerative heat exchanger as a basis, a method for designing heat exchangers to supply preheated air for open cycle magnetohydrodynamic power generation systems was developed. Design information and significant performance trends for multiple unit MHD air preheater systems were explored using a digital computer model which simulated operation of a cored brick regenerative heat exchanger. Thermal-hydraulic designs using numerous variations of core geometry and cycling parameters were completed to meet flow and temperature specifications of a typical full scale air preheater system. Unique values for flow rates, heat exchanger core sizing and ceramic mass requirements were calculated for each of these variations using criteria of limited thermally induced stress in the ceramic, specific discharge temperature for the preheated air stream and limited blowdown exit temperature droop.

Simulations using variations in tube roughness show minimal difference in total ceramic mass requirements. The model was used to determine the sensitivity of an air preheater performance to variation in flow and geometric parameters. Thermal operational characteristics of a cored brick heat exchanger test facility are predicted for several variations in flow rates and total cycle times.

Chapter I

INTRODUCTION

An important component of proposed coal-fired open-cycle magneto-hydrodynamic (MHD) power plants is the high temperature air preheater. High cycle efficiencies associated with MHD depend on passing a sufficiently high temperature, ionized, combustion gas stream through the magnetic field of the MHD generator channel. The combustion of coal and ambient air, without the benefit of preheated air or enrichment with oxygen will not produce a gas stream hot enough to operate the MHD generator channel at high efficiencies.

Cored ceramic brick regenerative heat exchangers are presently being considered as a means of preheating air for combustion with coal in MHD systems. The air preheater system in a full scale, coal burning, open cycle MHD system will represent a significant portion of the over-all system costs. The design of an efficient cored-brick regenerative air preheater facility with emphasis on the economical use of the ceramic core of the regenerator is a main area of consideration in this thesis. Reliability of the air preheater system is incorporated into the design procedure by limiting maximum values of thermally induced stress within the bricks.

The operation of a regenerative heat exchanger includes two basic functions. First, hot fluid passes through some intermediate energy

storage medium where energy in the form of heat is transferred from the hot fluid to the cooler storage medium. This phase is referred to as the reheat cycle. During the second operation, the blowdown cycle, heat which has been deposited in the storage medium is transferred to a cooler, counter-flow fluid stream. The cooler blowdown stream is heated and the regenerator storage matrix is cooled. The cycle is completed as the blowdown stream is terminated and the hot reheat stream once again flows into the opposite end to reheat the bed.

The energy storage medium can be of several types, but generally there are but two basic classifications. The first of these is the fixed bed or stationary type of regenerator, which operates on a cyclical pattern of alternate heating and cooling. The second method is the falling bed type regenerator, in which the heat storage medium consists of small particles of refractory material. The refractory particles or pebbles enter one of two vertical chambers where they are heated by a hot fluid. From this chamber the pebbles move into a second, usually lower, chamber where they give up their stored heat to a cooler gas. This heated gas leaves the second chamber at a higher temperature and the pebbles leave at a lower temperature than they entered. The pebbles then return to the upper chamber to again be heated and the process is repeated. The process operates continuously with no defined cycle periods, no reversals of flow and a constant

discharge temperature of the blowdown gas. The falling bed heat exchanger has advantages of delivering a constant temperature blowdown gas, requiring less valve operation, and using a less expensive heat storage medium. Its disadvantages include the problem of point to point contact between the pebbles which can present dusting and/or spalling problems, difficulties in maintaining a pressure difference between the streams, and in applications where the hot gas contains coal slag, the particles are susceptible to sticking together after they are coated with the slag.

The storage medium in the fixed bed regenerator is typically a refractory material which is selected for the temperature ranges it will encounter and the type of atmosphere to which it will be exposed. The core or matrix geometry of the refractory fixed bed regenerative heat exchanger may have three general configurations:

1) The matrix may be built from rectangular refractory bricks arranged into a number of unique patterns.
2) The matrix may be composed of a bed of spherical pebbles.
3) The matrix may be formed from cored ceramic with the holes aligned to form the flow passages.

This thesis considers only fixed bed regenerative heat exchangers with cored ceramic brick matrices. Typically the cored bricks have a hexagonal shape and the holes are arranged in a equilateral pattern as shown in Figure 1. The brick hole diameter, D, and the hole-to-hole

spacing, S, are two important parameters describing a brick configuration. Various experiments [18,20] have used holes as small as 6.35 mm (.25in.) to test cored brick air heaters. However, these regenerators were heated by clean burning fuels and were not subject to adhesion of seed and slag on the tube walls as are coal fired regenerators. Because of the non-abundance of clean burning fuels, coal is considered as the primary source for fueling MHD power systems. Typically the combustion gas stream is seeded with from 1 to 5% with potassium or cesium to enhance the ionization potential of the gases passing through the MHD channel. It is this mixture of coal combustion products and seed that pass through the air preheater during reheat in direct fired MHD cycles.

The MHD cycle may be designed to use a direct fired or indirect fired air preheater. Direct firing utilizes the exhaust gas stream from the MHD generator as the hot fluid during reheat. The energy of this stream is used to heat the regenerator matrix as is shown in Figure 2a. Indirect fired air preheaters operate by heating the regenerator matrix with a clean fuel, such as natural gas or gasified coal. The important consideration for using indirect fired preheaters is the absence of problems attributed to contamination by seed and the products of coal combustion on the heater matrix, and the build up of seed and slag on the matrix walls. An operating diagram of a typical open cycle MHD system using indirect firing of

air preheaters is shown in Figure 2b, with the steam bottoming cycle using the hot gases emerging from the MHD generator to superheat steam. The cooler gases then pass through a low temperature air preheater which has the advantage of being exposed to a cooler, less corrosive (because of condensation) seed and slag laden exhaust gas. The high temperature heater is not exposed to the coal combustion exhaust, but rather to the hot gases resulting from the residue free combustion of a clean fuel source. The main drawbacks of indirect fired preheater systems are associated with cycle efficiencies and fuel sources. Systems using direct fired preheaters, in theory, achieve an overall cycle efficiency 2 percent above the indirect fired system for a given preheat temperature [25]. Natural, clean burning fuel supplies are limited in quantity and gasification of coal requires a significant fraction of the total available heating value in a mass of coal.

With the exception of the interaction between the matrix material and the seed and slag laden products of high temperature coal combustion, open cycle MHD systems can effectively use a direct fired air preheater subsystem. Careful consideration must be given in the selection of materials which will withstand the combination of high temperatures and a corrosive atmosphere.

This thesis develops and analyzes thermal designs of cored ceramic brick heat exchangers suitable for open cycle MHD use.

Designs were completed which satisfy air preheater specifications for temperature and flow rates while operating below specified thermally induced stress levels in an effort to define core geometries providing efficient and economical use of the ceramic material.

Chapter II

Literature Review

The regenerative heat exchanger found its first use with Dr. Robert Stirling in 1816 who constructed a regenerator for a hot-air engine. Early analytical treatment of regenerator operation by Nusselt [12,13] produced solutions to the differential equations describing regenerators. His analyses have served as a basis for numerous analytical models simulating regenerators. Iliffe [11] simplified the solution of Nusselt somewhat, but the method involved the segmenting of the heater length into nodes, which, for each node required an hour of manual calculation to determine temperature changes and heat transfer.

Hausen [14,15,16] developed several methods for analyzing regenerative heat exchangers. In 1929 Hausen [14] developed the characteristic solution for equations describing an ideal regenerator which combined the heat transfer relations for the reheat and blowdown periods into a single relation which satisfied the reversal of flow direction and change in inlet temperature conditions. Hausen's "heat pole" method [15] for regenerators assumes a constant initial temperature distribution and utilizes a series of heat pole functions for describing transient temperature changes along an axially segmented bed. The heat pole functions are determined for both reheat and blowdown periods and a set of simultaneous equations results which is solvable for the

regenerator axial temperature distribution in each cycle. In 1942 Hausen [16] derived an exact mathematical expression for relating the mean ceramic temperature at a point along a regenerator to the surface temperature and the fluid temperature at that point using a modified heat transfer coefficient. This model for regenerator operation assumed constant gas and ceramic properties and a constant axial temperature gradient in the gas stream.

Hausen's, Nusselt's and Iliffe's methods were adaptable to solution without the aid of a computer but involved extensive calculations and lengthy mathematical manipulations.

Butterfield, et al [10] verified Hausen's [16] method with a digital computer analysis and presented a modified Hausen procedure which accounted for variations in heat transfer coefficients, variations in flow rates and specific heats and included radiation effects.

Contemporary thermal simulations of regenerative heat exchangers have taken advantage of the digital computer to make evaluation of regenerators more feasible. Wilmott's [1] primary work expressed the differential equations governing regenerative heat exchangers in a difference equation form. An algorithm was used to successively simulate each cycle from an arbitrary beginning until an equilibrium condition was reached. Wilmott, as Hausen and Butterfield also did, relates the heat transfer coefficient used in convection to the mean solid temperature rather than the surface temperature. Later, Wilmott

[3] incorporated into his model a variable mass flow of the working fluids to achieve a constant temperature stream both entering and leaving the regenerator. Wilmott found that using a variable flow operation reduces the effectiveness of the regenerator to transfer heat from the hot stream to the cold stream. Wilmott [2] also considered a three dimensional analysis of the regenerator which included the transverse as well as the axial temperature gradients in the matrix. Heat transfer in the transverse direction is also included in the ... method presented by Handley and Heggs [6] for simulating regenerators with matrix material laying parallel to a fluid flow, as in a cored brick heater. Reihman, Townes, and Mozer [31] have shown that detailed simulation of the transverse temperature distribution is not required for modeling cored brick regenerative heat exchangers.

Razelos and Lazaridas [8] developed a method adaptable to computer solution for calculating the transverse transient temperature distribution in a regenerative heat storage medium, relating the mean temperature from that distribution to the convective surface temperature, and modifying the heat transfer coefficient to account for resistance to heat transfer at the convective surface.

The model developed in this thesis extends Wilmott's method [1] to account for changes in local gas and ceramic temperature dependent properties, and utilizes the quasi-steady portion of the transverse temperature distribution of Razelos and Lazaridas [8] to relate the

surface temperature of the ceramic to the average ceramic temperature. Rather than modifying the heat transfer coefficient as Wilmott, and Razelos and Lazaridas did, the model used in this thesis relates the surface temperature to the average ceramic temperature and the local heat transfer coefficient for convection calculations.

Larsen et al [5] has proceeded with the solutions of Nusselt [12], Hausen [14], and Schumann [24] and developed a solution independent of initial ceramic temperatures and any time variation in inlet gas temperatures for finding fluid and solid temperatures at any time and location in a regenerative heat exchanger. Solution by this method involves approximating the arbitrary initial or inlet conditions as a number of linear segments and superimposing the results of the linear segments as a superposition type solution. The method uses tables and curves in the solution but does not require the use of a digital computer.

Equilibrium conditions are found without modeling successive cycles in the non-iterative technique presented by Edwards et al [4]. The method does not require complete digital simulation to determine temperature variations in regenerative heat exchangers; however, it does require considerable numerical approximation and matrix manipulation.

Regenerative heat exchangers have long been used in the iron and steel industry to economize the blast and open hearth furnace operations,

However, these heaters were mostly the type with a bulky matrix of stacked rectangular bricks. More recently, cored bricks have been developed in the aerospace industry to provide high temperature air for hypersonic wind tunnels and propulsion facilities. Various studies and experimental work [9,18,23,24] on high temperature cored brick storage heaters provide design techniques, thermal analyses and material evaluations, and demonstrate the ability of cored brick air heaters to provide preheat temperatures in excess of 2400 K.

Heywood and Womack [25] discuss the feasibility of various types of air preheaters and provide an overview of air heaters as they apply to MHD. Chojnowski et al [22] designed a regenerative heat exchanger of stacked rectangular bricks for preheating air in an open cycle MHD system.

To date, no directly coal-fired, cored brick regenerative heat exchangers are used in a full scale operation. Research effort is presently being directed towards applying the cored brick heat exchanger to high temperature energy conversion systems with emphasis on MHD [17,19,20,21]. Pilot heaters have been built to determine contaminant levels of an argon stream for a closed cycle MHD study [17], to define the reliability of an air preheater operating on a continual cycling basis [20,21], and to test both the corrosion of ceramics and the plugging of a flow stream by seed and slag [19,20,21].

Chapter III

Methods

3.1 Cored Ceramic Brick Regenerative Heat Exchangers

In this section, operating characteristics of cored ceramic brick heat exchanger systems are discussed. Relations between cycling times and the number of heat exchangers in each mode, and the causes of temperature droop in the exit gas stream are described. Design constraints and effects of minimizing cored brick hole diameter and S/D ratios are also included.

3.1.1 Operation of Heat Exchanger Systems

The purpose of the high temperature heat exchanger in a MHD generating system is to provide a constant mass flow of air which has been heated to a specified temperature. Preheat air at temperatures less than those specified tends to decrease the combustion flame temperature and results in a reduction in the overall efficiency of the MHD system.

The fixed bed heat exchanger must regularly undergo a regeneration period to maintain continuous operation. The MHD combustor must also receive a constant flow rate of heated air. Continuous operation requires a specific number of heat exchangers in the blowdown mode and a specific number in reheat at any given time. Theoretically, the minimum number of heat exchangers required would be two; one carrying the reheat gas and heating the matrix; the other carrying blowdown air

being heated by a hot matrix. However with an operation of this sort, maintaining a constant flow of constant temperature to the combustor would be difficult. Valving, pressurization and purging would have to take place instantaneously to insure continuous flow and the preheated air would be difficult to maintain at a constant temperature. The initial discharge air from the heat exchanger at the start of blowdown would be the highest temperature and would continually emerge at lower temperatures while the matrix energy was given up to the blowdown air. For precise control of flow and temperatures using a two heat exchanger system, auxiliary bypass streams would be required. Willmott [3] has shown that using a variable flow operation reduces the effectiveness of the regenerator to transfer that from the hot stream to the cold stream.

Regenerative heat exchangers experience changes in exit gas temperature with time. The magnitude of this variation for any cycle is called "temperature droop." The temperature droop from the beginning to the end of the blowdown cycle has three basic characteristics;

1. The longer the cycle time, the more droop there is.
2. The amount of droop is dependent upon the amount of ceramic heated and cooled.
    a) Large hole diameters increase ceramic mass and lead to less droop.
    b) Larger ratios of hole spacing to hole diameter (S/D) increase the mass of ceramic cooled and

heated and reduce the temperature droop.

3. The rate of heat removal from the ceramic bed affects the temperature droop. Higher blowdown velocities raise the heat transfer coefficient and the rate of heat removal. The ceramic is cooled faster and a greater temperature droop occurs.

The undesirable temperature droop can be offset by incorporating a larger number of heat exchangers in the preheater system. The amount of droop in each heat exchanger may be the same, but due to the number of heat exchangers cycling at sequenced times, the overall temperature droop can be reduced. This effect is shown in Figure 3.

A system of heat exchangers for preheating air would consist of a quantity, NR, of regenerators in the reheat mode, and a quantity, NB, in the blowdown mode at any given time. There will be a quantity, NS, of heat exchangers which are neither in the reheat nor the blowdown mode at a given time, but are in a transition period between the two. During this period, valving, purging, or pressurization may be occurring in the heat exchangers. The total number of heat exchangers in operation is then N_{tot} = NR + NB + NS. The value of NS will generally be two regenerators, one having finished the reheat mode and preparing for blowdown, the other following blowdown, before reheating.

The heat exchangers will undergo cycle changes progressively with a time delay equal to the switchover time STI seperating cycle changes. The number of heat exchangers NR will reheat for a specific time RTI,

and NB will be in the blowdown mode for a time BTI, while NS preheaters are in the switchover mode for a time STI.

As an illustrative example, assume there are 6 heat exchangers in reheat, 4 in blowdown and 2 in switchover modes. The ratio of reheat time to blowdown time must be the same ratio as NR/NB;

$$\frac{RTI}{BTI} = \frac{NR}{NB} = \frac{6}{4}$$

In this example, use RTI = 600 seconds and BTI = 400 seconds. In order to maintain 6 heat exchangers in the reheat mode and 4 in the blowdown mode it is necessary for there to be 6 switchovers during a reheat period or 4 during a blowdown period. Then;

$$STI = \frac{RTI}{NR} = \frac{BTI}{NB}$$

or in this example, STI = 600/6 = 100 seconds. An operational diagram for this system is shown in Figure 4. As the figure shows, for our example, there are 12 total operational heat exchangers, cycling at staggered times with a ratio of RTI/BTI = 6/4 and NR/NB = 6/4 at any time. At the time, t shown in the figure, heat exchangers 2,3,4,5 are in the blowdown phase, 7,8,9,10,11 and 12 are reheating while 1 and 6 are undergoing a switchover process. It is seen that the time lag between consecutive heat exchangers is equivalent to the switchover time, STI. To maintain flow continuity and insure equivalent conditions, the heat exchangers must be of identical size, with the same number of flow channels in each cored matrix. Equations for determining flow areas,

number of flow channels and velocity relations for reheat and blowdown are found in Appendix I.

3.1.2 Design Constraints

The cored ceramic bricks comprising the heater matrix of a direct fired cored brick regenerative heat exchanger in an open cycle-coal burning MHD power plant will be subjected to the hot, corrosive, seed and slag laden exhaust gases emerging from the MHD generator channel. High temperatures and a temperature accelerated corrosive attack of the seed and slag combine to make ceramic material selection for the cored bricks a principal task when designing MHD air preheaters. This thesis does not devote itself to material choice, but rather to specifying operational parameters and determining heat exchanger sizing and flow criteria. Numerous studies have been made which test different candidate materials for application in a coal burning, MHD plant air preheater system [26,27,28,29,30].

The presence of coal slag from the combustor process and the addition of a seed material to the MHD stream to increase the gas ionization introduce the probability of seed and slag deposition on the air preheater flow hole walls. To date, there are no coal fired cored brick regenerative heat exchangers in operation, so information concerning buildup of matter on tube walls is primarily from small scale experimental results [19] and simulations [7]. There is general agreement that small diameter holes (near 20 mm) should be avoided when using

a reheat gas laden with coal combustion products and seed, but a lower limit has not yet been determined and this thesis does not attempt to define a minimum hole diameter. However, the probability of plugging of holes or at least flow restriction by the adherance of seed or slag on the the tube walls is recognized and no extreme reductions in hole size are considered in the design process to reduce heat exchanger mass.

Nevertheless, the important design criteria of minimum possible ceramic mass is approached by using smaller diameter holes as is shown below. The major resistance to heat transfer is located at the convective surface, so by raising the convective surface area, a more effective heat exchanger results. The ratio of convective surface area to ceramic volume in the cored brick is inversely proportional to the hole diameter, or

$$\frac{A_{conv}}{Vol} = \left(\frac{1}{D}\right) \frac{1}{(S/D)^2 \cos(\pi/6) - 1/4}$$

From this equation it is seen that cored bricks with smaller diameter holes have a larger convective area to volume ratio and can transfer heat between the ceramic and the gas streams more effectively than large hole bricks, yet the plugging problem exists and is more severe with the smaller holes. Cored brick regenerators with large hole diameters can also provide high temperature preheated air, have a lower expectancy of plugging and exhibit less pressure drop along the flow stream. Although some pressure drop is acceptable, a minimum pressure

drop has the advantage of reducing auxiliary compressor and pumping requirements.

The equation in the previous paragraph also shows the dependence of the convection surface area to volume ratio upon the hole spacing to diameter ratio (S/D). Reducing the S/D ratio decreases the ceramic volume surrounding each hole and thereby increases the A_{conv}/Vol ratio. Problems resulting from a reduction in S/D include an increase in the blowdown exit temperature droop over a specified cycle time, a decrease in the average exit temperature for a specific cycle time, and anticipated increased fabrication difficulties arising from the reduction in web thicknesses. Advantages of smaller S/D are a more effective heat-transfer mechanism, a smaller total ceramic mass requirement, and smaller thermal stress levels for equal mass flow rates (this occurs as a result of smaller temperature differences between the convective surface and average ceramic temperatures).

Design trends then suggest that reductions in heat exchanger masses and a more effective mass use are obtained by decreases in hole diameter and/or decreases in the S/D ratio. The extent of these decreases is limited by the problems of slag buildup, pressure drops, fabrication difficulties and excessive blowdown exit temperature droop.

3.2 Lumped Mass Model

Included in this section are a discussion of the lumped mass model computer code which was formulated to simulate the thermal-hydraulic operation of a cored brick regenerative heat exchanger. The methods of analysis and assumptions used in the development of finite difference equations for the lumped mass code are presented as well as heat transfer correlations and equations for determining thermally induced stress in the ceramic. Also included is a discussion of the operation of the lumped mass code.

3.2.1 Assumptions and Analysis

The operation of a cored brick regenerative heat exchanger can be modeled with the aid of a digital computer. Various types of computer models can be prepared to simulate the heat exchange within the core and predict ceramic and gas temperature distributions, stress profiles, as well as local stream velocities, pressure changes and average discharge temperatures.

This section presents a model which is useful in the design of cored brick regenerative heat exchangers. The thermal analysis simulates the operation of a full scale heat exchanger by analyzing a single cell within the exchanger. The cyclical operation of the cored brick regenerative heat exchanger includes storage of energy during a reheat cycle when a hot gas flows through the parallel holes in the cooler regenerator matrix, and withdrawal of energy during a blowdown cycle

when energy in the storage matrix is transferred to a cooler counter-flow stream. Between reheat and blowdown is a set time for valving operations, and the pressurization or purging of the heat exchanger. The total regenerator cycle has these four periods; a reheat followed by a switching period, then a blowdown followed by another switching period. A computer simulation must model each operation over full duration of its cycle for the length of the heat exchanger. The large mass flows through the cored brick heat exchangers for preheating air in MHD power generation will dictate heat exchangers with large numbers of flow cells (ceramic enclosed flow streams). A computer model which examines the thermal-hydraulic operation of a typical cell in a cored brick heat exchanger was developed [31], which, by the symmetrical arrangement of the holes in the regenerator core, can be used to simulate the operation of the entire regenerative heat exchanger core.

Because of the symmetry between the cells in the heater matrix, adiabatic surfaces are located at points which are equidistant between the hexagonally patterned holes. The adiabatic surface characterizes the point between holes where the temperature gradient becomes zero and as shown in Figure (1b) is a hexagonal surface.

The computer model for simulating the thermal behavior of the cell employs the primary assumption that the temperature of the ceramic web between the holes will be uniform enabling the ceramic temperature to be averaged and thus to be characterized by the

average lumped temperature. This averaging of the ceramic temperature reduces the thermal analysis from a two dimensional problem to a one dimensional problem where only the axial temperature is calculated for the ceramic. The "lumped mass" model further assumes that the actual hexagonal adiabatic surface in the ceramic surrounding each hole can be represented by a cylindrical adiabatic surface encompassing the same ceramic volume (Figure 1b). The validity of this representation is supported by a nodal thermal analysis of the material surrounding the flow hole [31].

The average lumped temperature of the ceramic is determined by integrating the radial temperature distribution of the ceramic over the area between the flow hole and the cylindrical adiabatic surface. This radial temperature distribution in the circular tube is determined from the differential equation for heat flow in cylindrical coordinates,

$$\frac{\partial^2 T}{\partial r^2} + \frac{1}{r}\frac{\partial T}{\partial r} - \frac{1}{\alpha}\frac{\partial T}{\partial t} = 0 \qquad (1)$$

with the boundary conditions being an adiabatic outer surface and a convective heat flux at the inner surface, or

$$k\frac{\partial T}{\partial r} = -Q \qquad \text{at } r=a \qquad (1a)$$

$$\frac{\partial T}{\partial r} = 0 \qquad \text{at } r=b \qquad (1b)$$

The method of solution for equation (1) is found in Appendix II. The quasi-steady state (ignoring transients) temperature distribution across the ceramic annulus is

$$T(r,t) = \frac{Q\ a\ b^2}{k_c(b^2-a^2)}\left[\frac{r^2}{2b^2} - \ln\left(\frac{r}{a}\right) + \frac{2\ \alpha\ t}{b^2}\right] + C_5 \qquad (2)$$

This radial temperature distribution is not considered in detail by the lumped mass model, but is used;

1) to determine the average temperature in the ceramic
2) to determine the convective surface temperature at r=a, and to relate that temperature to the average ceramic temperature.
3) as a part of the thermal stress calculations in the ceramic.

The average ceramic temperature, or lumped temperature, found by integrating equation (2) over the area between r=a and r=b is

$$T_{avg} = \frac{Q\ a\ b^2}{k_c(b^2-a^2)}\left[\frac{b^2+a^2}{4b^2} - \frac{b^2}{b^2-a^2}\ln\left(\frac{b}{a}\right) + \frac{1}{2} + \frac{2\ \alpha\ t}{b^2}\right] + C_5 \qquad (3)$$

This temperature is used in the finite difference equations to characterize the temperature of an entire ceramic node, is used in calculations for heat conduction in the axial direction, and is used to calculate changes in internal energy of the ceramic.

Rather than using the lumped ceramic temperature to find the temperature difference between the ceramic and the gas stream in convection calculations, a convective surface temperature of the ceramic was

determined by evaluating equation (2) at r=a. Although differences between the wall temperature and the lumped temperature are not large, error in simulating heat transfer by convection is reduced if the wall temperature is used. From equation (2), the inner surface temperature, T_a, is

$$T_a = \frac{Q\,a\,b^2}{k_c(b^2-a^2)}\left[\frac{a^2}{2b^2} + \frac{2\,\alpha\,t}{b^2}\right] + C_5 \qquad (4a)$$

To eliminate the need for a two dimensional temperature analysis of the ceramic necessary to determine this convective surface temperature, T_a is expressed in terms of the average ceramic temperature, T_{avg}, from equation (3), or

$$T_a = T_{avg} + \frac{Q\,a\,b^2}{k_c(b^2-a^2)}\left[\frac{a^2}{2b^2} - \frac{b^2+a^2}{4b^2} + \frac{b^2}{b^2-a^2}\ln\left(\frac{b}{a}\right) - \frac{1}{2}\right] \qquad (4b)$$

Calculation of thermally induced stresses in the ceramic requires knowledge of the average temperature of the ceramic from equation (3) and the ceramic temperature of the location where the stress is to be calculated from equation (2). The formulation of the thermal stress relations are discussed in section 3.2.4.

The lumped mass model utilizes a finite difference scheme to calculate the temperature distributions in the ceramic and fluid and their variations with time. Finite difference equations developed for both the fluid stream and the ceramic tube permit an explicit solution which steps axially over the length of the heat exchanger and steps with time

over the duration of each reheat or blowdown cycle. The lumped mass model also simulates a switchover period and a reversal of flows between cycles. Consecutive cycles are simulated until cyclic equilibrium conditions are reached.

For large heat exchangers with many flow channels, the lumped mass model simulates their operation well. Heat transfer between adjacent channels is negligible in large heat exchangers and the cylindrical representation of the adiabatic surface between the holes provides a suitable method for reducing the complexity of the mathematical solution while retaining an accurate model. For small heat exchangers where an appreciable fraction of the heat entering the ceramic is lost to the insulating material, heat transfer between adjacent tubes is no longer negligible and accuracy of the model is reduced.

The lumped-mass model was developed utilizing the assumption that the temperature gradients used in calculating axial conduction in the ceramic may be determined using ceramic temperatures from the previous time step. This assumption is justified if time steps are sufficiently small. The use of this assumption saves computational complications by converting a system of dependent equations into a series of equations applicable to an explicit solution.

Two additional assumptions involve methods of heat transfer in the fluid. These state that the change in energy transported in the moving fluid is much greater than either the axial conduction of heat within

the gas stream or the transient storage of energy in the gas stream. These assumptions are expressed as

$$k_g A \frac{\partial T_g}{\partial z} << \dot{m}_g C_{pg} \Delta z \frac{\partial T_g}{\partial z} \tag{5}$$

and

$$\rho_g C_{pg} A \Delta z \frac{\partial T_g}{\partial t} << \dot{m}_g C_{pg} \Delta z \frac{\partial T_g}{\partial z} \tag{6}$$

Finally, the lumped mass program assumes heat transfer by radiation between the ceramic and the gas stream, since convection is taken to be the only mechanism.

3.2.2 Development of the Finite Difference Equations

The finite difference equations used in the lumped mass model were developed by making energy balances on elemental lengths of the heat exchanger tube and of the fluid stream. Energy balances on the ceramic cylinder used the lumped ceramic temperature from equation (3) for energy storage and axial conduction in the ceramic, and the convective surface temperature, T_a, from equation (4) for determining convection. The length of the tube is divided evenly into segments as shown in Figure 5, with the temperature of an entire segment being represented by the lumped temperature at its center. The gas stream is divided into the same length segments with nodal points corresponding to the ends of the ceramic elements as shown in Figure (5). Selection

of the length step size and the time increment used in the lumped mass model is discussed in Appendix VI.

Axial temperature gradients in the ceramic are approximated using the ceramic temperatures of the adjacent elements. As mentioned previously, axial conduction in the ceramic is included in the difference equations by using the ceramic temperature gradient from the previous time step. If short enough time steps are selected, the change in temperature gradient through that time change will be small.

The energy balance on the ceramic element includes axial conduction, convection and a storage term. The convective heat transfer is modeled using a dimensionless coefficient, α_6, which relates the wall surface temperature to the lumped ceramic temperature and corrects for heat transfer resistance at the convective surface. Local material properties are determined using the local temperature at the nodal point. The finite-difference equation resulting from energy balance done on the ceramic element is:

$$T(j,2) = \left[1 - 2\alpha_3 - \frac{\alpha_1}{1+\alpha_6}\right] T(j,1) + \alpha_3 \left[T(j-1,1) + T(j+1,1)\right]$$

$$+ \frac{\alpha_1}{2(1+\alpha_6)} \left[TG(j) + TG(j+1)\right] \qquad (7)$$

In this equation, the dimensionless parameter α_1 is the product of the local Biot and Fourier moduli and includes the relative magnitudes of surface convection and internal conduction resistance to heat transfer

in the ceramic;

$$\alpha_1 = \frac{2\ \alpha\ \Delta t}{(b^2-a^2)} \frac{h\ a}{k_c} = 2\ Bi\ Fo \tag{8}$$

The α_3 parameter is the ratio of the rate of heat transfer by axial conduction in the ceramic to the rate of energy stored;

$$\alpha_3 = \frac{k_c\ \Delta t}{\rho_c C_{pc}\ \Delta z^2} \tag{9}$$

The inner wall surface temperature of the ceramic used for convection is related to the average ceramic temperature by the dimensionless parameter

$$\alpha_6 = \frac{h\ a\ b^2}{k_c(b^2-a^2)} \left[\frac{a^2}{2b^2} - \frac{b^2+a^2}{4b^2} + \frac{b^2}{b^2-a^2} \ln\left(\frac{b}{a}\right) - \frac{1}{2} \right] \tag{10}$$

The energy balance performed on the gas element includes the heat transfer between the gas and ceramic due to convection and the energy transported in the fluid stream. Changes in energy from both transient storage in the gas element and conduction in the gas stream and radiative heat transfer are assumed negligible. As before, the convection between the gas stream and the ceramic is found using the modified surface temperature. The finite difference equation for determining axial variations in the gas stream developed from the energy balance on the gas element is

$$TG(j+1) = TG(j) \frac{\left[1 - \frac{\alpha_2}{2(1+\alpha_6)}\right]}{\left[1 + \frac{\alpha_2}{2(1+\alpha_6)}\right]} + T(j,1) \frac{\left[\frac{\alpha_2}{1+\alpha_6}\right]}{\left[1 + \frac{\alpha_2}{2(1+\alpha_6)}\right]} \tag{11}$$

The dimensionless α_2 parameter compares the magnitudes of surface convection to the heat capacity of the moving fluid.

$$\alpha_2 = \frac{2 \pi a h \Delta z}{\dot{m} C_{pg}} \qquad (12)$$

The development of the nodal equations for both gas and ceramic is expanded in Appendix III. The lumped-mass model uses local gas and ceramic properties which vary with temperature. Relations for temperature varying properties were developed using a least-squares curve fitting technique and are incorporated into the model. These functional properties include thermal conductivity, viscosity, specific heat and Prandtl number for the gas streams and the thermal conductivity of the ceramic. Fluid properties vary between reheat and blowdown as does the composition of the reheat and blowdown gases. The reheat stream in the model is a gas formed by the products of combustion of coal and air. The blowdown stream is air. The ceramic properties and the functional gas properties are developed and listed in Appendix IV.

3.2.3 Heat Transfer Correlations

The heat transfer correlation used in the lumped-mass model accounts for entry length effects and pipe roughness effects. The Nusselt number correlation is calculated using local instantaneous Reynolds and Prandtl numbers. Data from Seider and Tate [32] was fitted to a Nusselt number correlation presented by Hausen [33] which

incorporates entrance conditions for smooth pipe flow. This equation does not account for pipe roughness so the Hausen equation was further corrected by the ratio of Nusselt numbers for rough and smooth pipes as determined by a correlation given in The Handbook of Heat Transfer [34] and friction factors obtained from Schlicting [35]. The resulting equation used in the lumped-mass model is

$$Nu = 0.131\,[Re^{2/3} - 138]\,Pr^{1/3}\,[1 + \tfrac{1}{3}(\tfrac{2a}{X})^{2/3}]\,(\tfrac{f_r}{f_0})^{0.457} \qquad (13)$$

The transition from laminar to turbulent flow is assumed to occur at Re = 2242. It is at this value of Re that equation (13) predicts the Nusselt number to have a laminar flow value of

$$Nu = 4.364 \qquad Re < 2242 \qquad (14)$$

The friction factor is calculated for local conditions from Schlicting [35] as the solution to

$$\frac{1}{\sqrt{f}} = 1.74 - 2\log_{10}\left[\frac{k_s}{a} + \frac{18.7}{Re\sqrt{f}}\right] \qquad (15)$$

For laminar flow the friction factor is

$$f = 64\,Re^{-1} \qquad Re < 2242 \qquad (16)$$

The development of heat transfer correlations is given in Appendix V.

3.2.4 Calculation of Thermal Stresses in Cored Ceramic Bricks

The brittleness of ceramic materials causes thermal stress failure to be a major limitation when using ceramic materials in heat exchangers. In this thesis the limitation of thermal stresses was an important constraint in the air preheater designs and in the establishment of flow conditions and operating procedures.

Thermal stresses are caused by restraint of thermal expansion and/or contraction. This restraint may be external where expansion of the entire brick is restrained by an outer body when the brick is heated, or it may be internal where thermal expansion or contraction is obstructed by neighboring material within the brick. The thermal stresses arising from external restraint are not a serious design problem and are easily avoided by providing sufficient space for the thermal expansion.

The thermal stresses resulting from internal restraint can not be relieved by providing space for expansion, but depend upon the temperature distribution within the material and the material properties, specifically the coefficient of thermal expansion, Poisson's ratio and the modulus of elasticity for the material.

Three distinct temperature distributions exist in a cored ceramic brick regenerative heat exchanger. They are the axial and radial temperature distributions extending over the heater "body" and the "localized radial" temperature distribution in the ceramic "web" surrounding the flow holes.

The axial temperature distributions in the ceramic flow tube for a typical thermal design case are shown in Figure 6. These figures show the average temperatures of the tubes at the beginning and end of each cycle. The spacing between the curves indicates the maximum temperature variation at the given location in the ceramic bed.

Heat loss in the radial direction through the insulating material causes the cored brick at the outer edge of the heat exchanger in contact with the insulation to be cooler than those in the center of the bed and creates a radial temperature distribution in the heat exchanger. The thermal stresses produced by the vertical and radial temperature distributions are referred to as "body" stresses because they result from temperature gradients which cover the entire body of the heat exchanger. The body temperature distributions and stresses are related primarily to the length and diameter of the bed, coupled with the insulation design and heater flow conditions. Body stresses can be reduced by decreasing the dimensions of individual bricks in directions parallel to the temperature gradients. As an example, shorter bricks can be used at the top of the heat exchanger where axial temperature gradients are greatest to reduce axial thermal stresses.

The third source of thermal stresses are in the individual webs between the holes. During reheat the bricks are heated at the surface of the ceramic and during blowdown they are cooled from the surface. The flow of gas through the holes and the convection between the fluid

stream and the surface produce temperature gradients in the webs. The stresses caused by temperature distributions in the webs are "web" stresses and are dependent on the flow conditions in the holes. Web stresses caused by the reheat gas stream are much lower than those caused by the blowdown air because the rate at which the bed is heated is much less than the rate at which the bed is cooled. The low rate of heating allows for more radial conduction in the ceramic and a more uniform temperature distribution. During reheat, the tube surface is heated faster than the interior creating compressive web stresses at the tube surface and tensile stresses inside the web. The opposite is true for blowdown. The cooler blowdown air stream cools the tube surfaces and creates tensile stresses at the surfaces of the holes. Condition of tensile stresses is more important and more apt to lead to failure since the tensile strength for ceramics is considerably lower than their compressive strength.

Body stresses caused by the vertical and horizontal temperature distributions in the heat exchanger can be controlled by insulation design and individual brick sizing and are not analyzed in the lumped mass model. Web stresses were calculated in the lumped mass code using the idealized model by representing the hexagonally patterned holes by a nest of tubes, each with a circular hole and a hexagonal outer surface. The hexagonal outer surface was further simplified to an equivalent cylindrical surface surrounding the same volume of ceramic.

From Timoshenko and Goodier, [37], the maximum elastic thermal stresses for circular tubes are axial and are given by

$$\sigma(r) = \frac{\beta E}{1-\nu} \left(T_{avg} - T(r)\right) \qquad (17)$$

T_{avg} is the average ceramic temperature at an axial nodal position as determined from equation (3) and $T(r)$ is a ceramic temperature at a radial position as determined by equation (2). The most critical stresses determined by equation (17) are the thermal stresses at the inner wall, $r = a$, where heating by the reheat stream or cooling by the blowdown stream causes the greatest difference between T_{avg} and T_a. Here the stress is

$$\sigma(a) = \frac{\beta E}{1-\nu} \frac{Q}{k_c} \frac{a\,b^2}{b^2-a^2} \left[\frac{b^2-a^2}{4b^2} - \frac{b^2}{b^2-a^2} \ln\left(\frac{b}{a}\right) + \frac{1}{2} \right] \qquad (18)$$

In equation (18), Q [W/m^2] is the rate of energy entering a ceramic node and is positive during reheat and negative during blowdown. The geometric quantity in brackets has a negative value resulting in a compressive stress during reheat and a tensile stress during blowdown. This is expected, as during blowdown the surface is exposed to cool blowdown air and contracts, developing tensile stresses at the surface of the hole. During reheat, the surface expands as it is heated and develops compressive stresses.

The thermal stress analysis used in the lumped mass model is based only on elastic stresses and strains. It does not consider effects if

yielding or creep occurs. The maximum tensile stresses calculated in the lumped mass model are compared with limits for thermal stress which are specified in design criteria. Designs presented in this thesis were developed by varying flow rates to achieve stress levels which are bounded by the limits set in the thermal design criteria. Designs were made for two maximum tensile thermal stress levels of 13.79×10^6 Pascals and 34.47×10^6 Pascals. To date, information describing thermal stress limits in ceramic materials is limited. The tensile strength of the ceramic was not used for the thermal stress limit because the thermal stress limit will be dependent on the surface finish of the holes, material density, and temperature. There is also evidence that seed and slag coatings on the tube wall effect the ability for the ceramic to resist cracking. More precise definition of maximum allowable thermal stresses in the cored brick regenerative heat exchangers remains an area for further study.

3.2.5 Operation of the Lumped-Mass Model Computer Code

The lumped-mass model computer code was developed to determine cyclic equilibrium conditions in a cored brick regenerative heat exchanger. The code computes the axial temperature profile for a gas flowing through a ceramic tube and the axial temperature distribution in the ceramic tube. Calculations are done explicitly, stepping in both time and axial distance along the tube. The results obtained from

modeling the single tube define operating characteristics of the matrix of flow tubes making up an entire heat exchanger. The lumped-mass model simulates flow of a hot gas flowing downward through a vertical flow tube and calculates the amount of energy entering the tube wall from the gas. This, the reheat phase or cycle lasts for a specified period of time. At the end of the reheat cycle the code simulates a period to be used for valve switching, pressurization or purging between cycles, where flow in the channel ceases and heat transfer in the ceramic is by axial conduction alone. Following this switchover period, the model simulates flow of a cooler air stream entering the bottom of the heat exchanger and calculates the heat transfer from the hot bed and the heating of the cooler "blowdown" stream. The blowdown period is followed by successive reheating and blowdown periods seperated by the switchover periods.

Inlet gas temperatures and pressures for each cycle, as well as the cycling times are required input variables for the lumped-mass model. The temperatures and pressures are defined for various MHD generator systems by Corman, et al, [36] in the General Electric E.C.A.S. Report, which also includes total mass flow rates for the reheat and blowdown gas streams and exit temperatures for each stream (Fig. 7).

A flow geometry consisting of bed length, L, hole diameter, D, hole-to-hole spacing, S, and the number of heat exchangers in each mode of operation, NR and NB, must be specified for operation of the lumped-mass model. Either of the inlet velocities (V1 or V2) must also be specified. The second inlet velocity is determined from the geometry, mass flow rates and the first velocity as indicated in Appendix I, equation A1.10.

An initial arbitrary ceramic temperature distribution serves as a starting point for the model which simulates operation of successive cycles from this initial distribution until an equilibrium condition is achieved, where the total heat transfer during a reheat cycle equals the total heat transfer of the following blowdown cycle and temperature variations between consecutive reheat cycles or consecutive blowdown cycles are unchanging. At this point temperature distributions in both ceramic and gas streams, average exit gas temperatures, thermal stresses in the ceramic and heat transfer values are printed.

3.3 Design Procedure

Included in this section are a discussion of the procedures used to complete heat exchanger thermal designs and the specific design parameters required to be met in completing the designs. A Newton-Raphson iterative technique for determining design parameters was incorporated into the lumped mass model and is described in this section.

3.3.1 Selection of Design Conditions

Two major considerations dictating the success of regenerative air preheater system for open cycle magnetohydrodynamics are its ability to provide the air at prescribed temperatures and reliable operation over extended periods. Preheat temperatures less than those prescribed for an MHD cycle tend to lower the efficiency of the generation system and raise the costs of the power generated. Interrupted operation of an air heater due to failure of its core by thermally induced stress cracking is a costly design mistake which is avoidable by proper selection of flow rates to reduce the maximum thermal stress level experienced in the cored bricks.

The two requirements to be met in designs developed using the lumped mass model are then a maximum thermal stress level and a prescribed temperature for the blowdown discharge air. Because ceramic materials are brittle and fail in tension rather than compression, the maximum stress limit was further specified as the maximum positive, or

tensile, thermal stress acceptable in the ceramic. Because the limit is not clearly defined for thermal stresses in ceramic, designs were completed using two parametrically set limits. Designs with "high" stress limits have maximum thermal stresses of 34.47×10^6 Pascals and designs with "low" stress limits have maximum thermal stresses of 13.79×10^6 Pascals.

The prescribed blowdown air discharge temperature, which is equal to the required temperature of the preheat air entering the combustor in open cycle MHD, was chosen as a design criteria because of its importance in elevating the flame temperature in the combustor and increasing MHD cycle efficiency. During the blowdown cycle, the blowdown air discharge temperature from the heat exchanger exits initially at a high temperature which continually decreases throughout the blowdown cycle as the stored heat in the core is diminished. The final exit temperature at the end of the blowdown cycle may be considerably lower than the initial exit temperature. By addition of a number of heat exchangers cycling in sequence, the discharge temperature over the blowdown periods is averaged. This average temperature is approximated by averaging the discharge air temperature of a single tube over a blowdown period. This is calculated from the results of the lumped mass model. The temperature criteria for heat exchanger designs specifies the average blowdown exit temperature must be equal to the value required for the preheat air temperature in an open cycle MHD generator system.

Because of the sensitivity of the MHD generator channel performance to temperature fluctuation, considerable variation in the combustion air preheat temperature can not be tolerated. The maximum blowdown exit temperature droop acceptable in the thermal design cases was 100 K. Designs exibiting temperature droop greater than 100 K were not acceptable and are not presented in this thesis.

The exit temperature of the reheat air was not used as design criteria as this temperature is fairly dependent on the value of the blowdown temperature and can not be varied significantly without causing the average blowdown temperature to diverge from its required value. The reheat gas exit temperature is not vital to the operation of the MHD generator but has a secondary effect associated with a steam bottoming plant.

3.3.2 Newton-Raphson Method of Determining Design Conditions

The specified design condition to be met using the lumped-mass model is the average discharge temperature of the blowdown stream. While meeting this condition the maximum thermal tensile stress in the brick must be limited to the desired value. The average blowdown discharge temperature is calculated as the numerical average of the exit gas temperature at every time step over the duration of the blowdown cycle.

$$TEXIT = \frac{\Delta t}{BTI} \sum_{t=1\Delta t}^{BTI} TG(m)_t \qquad (19)$$

where $TG(m)_t$ is the blowdown gas temperature for time t at axial position m, the point of discharge. Typically the designs require an average blowdown temperature of 1644 K which is the air preheat temperature designated in the General Electric ECAS Base Case 1 for open cycle MHD [36].

The limit on the maximum thermal stress in the ceramic is a design constraint. Because ceramic materials are brittle and fail in tension rather than compression, the maximum tensile thermal stress (positive value in the thermal stress equations) is used to the limit set for thermal stresses. Generally this maximum stress occurs at the beginning of the blowdown period. As developed in section 3.2.3, thermal stresses at the inside surface of the ceramic tube are found using results from Timoshenko and Goodier [37]

$$\sigma = \frac{\beta E}{1-\nu} (T_{avg} - T_a) \qquad (20)$$

The limits for maximum thermal stress in ceramic are not clearly defined, so in designing the cored brick regenerators two values for maximum allowable stresses were used. "Low" stress level designs used a maximum stress value of 13.79 MPa, and "high" thermal stress level designs used a value of 34.47 MPa.

A modified Newton-Raphson iterative technique was used as a convenient method of accurately meeting the design conditions with the lumped-mass model. This method was incorporated into the model and presented a means for valid comparison between designs. Each particular design is based on a fixed core geometry, fixed NR/NB ratio, fixed total cycle time (RTI+BTI), and set flow conditions (pressures, inlet fluid temperatures, mass flow rates) for both reheat and blowdown cycles. What remains to be found is the bed length L and the fluid velocities V1 and V2. Knowing these, the sizes of the heat exchangers can be determined as outlined in Appendix I. The inlet blowdown velocity, V2, is uniquely determined from the reheat velocity and core configuration as shown in Appendix I. Therefore L and V1 are the only two design parameters to be determined. The proper combination of L and V1 result in the desired values TEXIT and σ_{max}. Stated in functional form

$$TEXIT = TEXIT[L,V1] \qquad (21)$$

$$\sigma_{max} = \sigma_{max}[L, Vl] \tag{22}$$

A specific combination of L and Vl will give a unique TEXIT and σ_{max}. An increment in L, from L_1 to L_2, holding Vl constant changes TEXIT and σ_{max}. These changes may be approximated as

$$\frac{TEXIT_1 - TEXIT_2}{L_1 - L_2} = \frac{\Delta TEXIT_{1-2}}{\Delta L_{1-2}} \cong \frac{\partial TEXIT}{\partial L} \tag{23}$$

$$\frac{\sigma_{max_1} - \sigma_{max_2}}{L_1 - L_2} = \frac{\Delta \sigma_{max_{1-2}}}{\Delta L_{1-2}} \cong \frac{\partial \sigma_{max}}{\partial L} \tag{24}$$

Also, an increment in Vl from Vl_1 to Vl_3 using the initial bed length, L_1, will result in changes in $TEXIT_1$ and σ_{max_1} to values of $TEXIT_3$ and σ_{max_3}, or

$$\frac{TEXIT_1 - TEXIT_3}{Vl_1 - Vl_3} = \frac{\Delta TEXIT_{1-3}}{\Delta Vl_{1-3}} \cong \frac{\partial TEXIT}{\partial Vl} \tag{25}$$

$$\frac{\sigma_{max_1} - \sigma_{max_3}}{Vl_1 - Vl_3} = \frac{\Delta \sigma_{max_{1-3}}}{\Delta Vl_{1-3}} \cong \frac{\partial \sigma_{max}}{\partial Vl} \tag{26}$$

The Newton-Raphson method predicts the changes in the original L and Vl necessary to change the original TEXIT and σ_{max} to the required design values, by the simultaneous solution of the following equations for ΔVl and ΔL

$$\frac{\partial TEXIT}{\partial V1} \Delta V1 + \frac{\partial TEXIT}{\partial L} \Delta L = TEXIT_{design} - TEXIT_1 \quad (27)$$

$$\frac{\partial \sigma_{max}}{\partial V1} \Delta V1 + \frac{\partial \sigma_{max}}{\partial L} \Delta L = \sigma_{max_{design}} - \sigma_{max_1} \quad (28)$$

The partial derivatives are approximated in equations (23,24,25, and 26). $TEXIT_1$ and σ_{max_1} are values resulting from L_1 and $V1_1$, while the "design" values are those specified in the design case.

A procedure used in completing a design by finding unique values for the bed length and reheat velocity is then;

1. Define cycle conditions and preheat requirements.
   A. Reheat mass flow rate, blowdown mass flow rate
   B. Inlet reheat gas pressure and temperature
      Inlet blowdown are pressure and temperature
   C. Average blowdown air exit temperature (required preheat temperature for combustor) - $TEXIT_{design}$
2. Set parametric maximum thermal stress level requirement - $\sigma_{max_{design}}$
3. Specify flow conditions and core geometry
   A. Flow hole diameter - D
   B. Flow hole spacing to diameter ratio - S/D
   C. Number of heat exchangers in reheat mode at any time - NR
      Number of heat exchangers in blowdown mode at any time - NB
   D. Reheat time (RTI), Blowdown time (BTI), Switchover time (STI)

4. Initialize conditions

   A. Specify initial approximation for bed length - L_1

   B. Specify initial approximation for reheat velocity - Vl_1

   C. Set arbitrary initial ceramic temperature distribution

5. Run lumped mass code to determine equilibrium conditions

   A. Reheat and blowdown gas exit temperatures

   B. TEXIT - average blowdown air exit temperature

   C. Maximum thermal stress level - σ_{max} (generally at bottom of heat exchanger at entrance for blowdown air and at beginning of blowdown cycle)

6. TEXIT and σ_{max} are compared with design requirements.

   A. $TEXIT_{design} - TEXIT_1 = \Delta TEXIT$

   B. $\sigma_{max_{design}} - \sigma_{max_1} = \Delta\sigma_{max}$

   C. If these differences are great, steps 4, 5 and 6 may be repeated with alternative initial approximations.

7. Lumped mass code is run with original reheat velocity, Vl_1, and a bed length of L_2, slightly different than the original length L_1

   A. $\frac{\partial TEXIT}{\partial L}$ is determined according to equation (23).

   B. $\frac{\partial \sigma_{max}}{\partial L}$ is determined according to equation (24).

8. Lumped-mass code is run with original bed length, L_1, and a reheat velocity of Vl_3, slightly different than the original velocity Vl_1.

   A. $\frac{\partial TEXIT}{\partial Vl}$ is determined according to equation (25).

B. $\frac{\partial \sigma_{max}}{\partial V1}$ is determined according to equation (26).

9. Changes from the original approximations for bed length, L, and reheat velocity, V1, are determined by simultaneous solution of equations (27) and (28) for ΔL and $\Delta V1$.

10. New values of bed length and reheat velocity are determined.

    A. $L = L_1 + \Delta L$

    B. $V1 = V1_1 + \Delta V1$

11. Code is run with these new values of L and V1. Resulting TEXIT and σ_{max} are compared with required values.

    A. If differences are acceptable small, the designs are completed with these new values.

    B. If differences are unacceptably large, the new L and V1 are used as original approximations; steps 7-11 are repeated.

12. Designs exhibiting excessive blowdown exit temperature droop are discarded.

Generally, with a good initial approximation only one Newton-Raphson iteration is required. If the first approximation leads to large differences according to steps 6-A and 6-B, a manual re-approximation for the initial length and reheat velocity will result in less computational time required to find the correct values of L and V1 than repeated Newton-Raphson iterations.

The value of $\frac{\partial TEXIT}{\partial L}$ is usually positive; a longer bed length will increase the average blowdown exit temperature. The value of $\frac{\partial \sigma_{max}}{\partial L}$

usually is negative; thermal stresses are lower for longer beds. Higher velocities increase the heat flux from the ceramic and tend to raise the maximum thermal stress level, hence $\frac{\partial \sigma_{max}}{\partial V1}$ has a positive value.

The value of $\frac{\partial TEXIT}{\partial V1}$ is negative in the region where the reheat and blowdown streams are laminar and remains negative until the velocity is increased enough to bring the reheat stream into the turbulent region. As the streams enter the turbulent flow region, $\frac{\partial TEXIT}{\partial V1}$ becomes positive. In this region the increased heat transfer rate caused by increased velocity escalates faster than the mass flow rate. This trend continues until the effects heat transfer rate and the mass flow rate balance out. At this point, the increase in heat transfer rate caused by increased velocity is just enough to heat the additional mass flow and $\frac{\partial TEXIT}{\partial V1}$ becomes zero. The value of TEXIT has a maximum value for the flow geometry as shown in Figure 8. Above this point $\frac{\partial TEXIT}{\partial V1}$ is again negative and the mass flow rate increases faster than the ability of the ceramic to heat the stream.

Chapter IV

Design

4.1 Presentation of Designs

Thermal-hydraulic designs and operating conditions for cored brick regenerative heat exchangers are presented in this section. Included are designs for preheaters capable of supplying preheated combustion air for a full scale, coal fired, open cycle MHD generation system and operation simulations for a small scale cored brick heat exchanger to be used as a test facility. The designs were completed with the aid of the lumped mass digital computer code previously discussed.

Base Case 1 for open cycle MHD from the General Electric ECAS report [36] was used as the design basis for the full scale air preheater designs. Base Case 1 is a typical open cycle MHD cycle and was chosen to demonstrate expected MHD air preheater sizes, cycling characteristics and design procedures.

The designs presented indicate the heat exchanger sizing and operational information necessary to define a system capable of providing the preheated air stream designated in the ECAS Base Case 1 cycling diagram (Figure 7). This information includes:

1) hole geometry (hole diameter, hole spacing to diameter ratio, bed length)
2) bed size (number of holes, mass and volume of ceramic in the bed, radius of bed)

3) flow conditions (inlet pressures, temperatures, velocities for reheat gas and blowdown air streams, total mass flow rates for reheat and blowdown)

4) cycle information (reheat and blowdown cycle times, number of heat exchangers operating in reheat and blowdown).

For the test facility simulations, the hole geometry and bed sizing are considered fixed. Flow conditions and cycling information for a number of simulation cases are presented.

4.1.1 Designs for ECAS Base Case 1

Base Case 1 for open cycle MHD from the General Electric ECAS report [36] describes the operating conditions for a 2000 MWe MHD power plant. Base Case 1 was chosen as typical of open cycle MHD configurations utilizing direct heating of the high temperature air preheaters by the coal-air combustion products from the MHD channel.

Designs for heat exchangers capable of duplicating the flow rates and temperature ranges specified in ECAS Base Case 1 were completed with the aid of the lumped mass program. The designs were based on the ability to meet three basic criteria.

1) The average exit temperature for the blowdown stream as determined in the lumped mass model must equal the preheat temperature designated in Base Case 1, specifically,

$$TEXIT_{BD} = 1644 \text{ K}$$

where $TEXIT_{BD}$ is the average exit temperature over the duration of an equilibrium blowdown period.

2) The maximum thermally induced stress in the ceramic brick must not exceed a prescribed maximum value. Two maximum values were established. Designs with "low" maximum thermal stresses have a limit set at

$$\sigma_{max\ low} = 13.79\ MPa$$

Designs with "high maximum thermal stresses have a limit set at

$$\sigma_{max\ high} = 34.47\ MPa$$

3) Individual heat exchanger blowdown exit temperature droop must be less than 100 K.

From the cycle diagram (Figure 7) for ECAS Base Case 1, the high temperature air preheater is designated to operate with the additional specifications for temperature and flow of;

Reheat gas inlet temperature	= 1894 K
Reheat gas inlet pressure	= 112400 Pa
Reheat gas mass flow rate	= 138.2 kg/sec
Reheat gas exit temperature (avg.)	= 1478 K
Blowdown air inlet temperature	= 1122 K
Blowdown air inlet pressure	= 972200 Pa
Blowdown air mass flow rate	= 112.8 kg/sec

Blowdown air exit temperature (avg.) = 1644 K

The blowdown air inlet temperature is not given in Figure 7 but was determined from an energy balance on the two streams and found to be 1122 K. The reheat gas exit temperature calculated in the design simulations was not used as a design criteria because it was dependent on the value of the average blowdown exit temperature. Generally, the average reheat temperature attained a value of 1520 K, about 40 K higher than the Base Case 1 specification.

The designs presented in this section consider a variety of hole diameters, cycling times and ratios. Designs were completed using;

1) hole diameters of 19.05, 38.1 and 50.8 mm.
2) ratios of hole spacing to hole diameter (S/D) of 1.20, 1.40 and 1.60.
3) NR/NB ratios of 4/6, 5/5, 6/4, and 6/3.
4) total cycle times (RTI+BTI) of 1000, 2000 and 3000 seconds.
5) maximum thermal stress limits of 13.79 MPa and 34.47 MPa.
6) $TEXIT_{BD}$ = 1644 K.
7) Blowdown exit temperature droop less than 100 K.

The lumped mass model and the Newton-Raphson technique were used to determine unique values for the bed length and the inlet velocities which satisfy statements 5 and 6 above for combinations of D, S/D, NR/NB and RTI+BTI from statements 1,2,3 and 4 above which satisfy item 7. Figures 9 through 17 exhibit the bed lengths and inlet gas and air

velocities which satisfy the temperature and stress requirements for the various combinations of geometric and cyclic parameters. Table 1 lists the variables used in each of the Figures 9 through 17 and includes the stress limit used in each design. A wall sand grain roughness of 0.254 mm was chosen for the lumped mass model air preheater simulations of Table 1. Bed lengths and inlet velocities were determined for the two smooth wall cases shown in Table 2 to demonstrate the effect of wall roughness on heat exchanger sizing.

Figures 18 to 20 show the variation in total ceramic mass required for the acceptable core designs presented in Figures 9 - 17. This section of figures is classified according to hole diameter and maximum thermal stress. The total mass for the heat exchanger system is found by multiplying the mass of a single heat exchanger (equation (A1.14), Appendix I) by the total number of operational heat exchangers, or

$$\text{Mass}_{\text{total}} = \frac{\text{mass}}{\text{h.x.}} (NR + NB + 2)$$

From Figures 9 - 17 and Figures 18 - 20, characteristics for specific designs are found by selecting a hole diameter, S/D ratio and thermal stress limit from Table 1. From Table 1, the correct figure which corresponds to these conditions is identified. The number of heat exchangers in each mode is selected and the ratio of NR/NB is formed. The required length and inlet velocities are found as the ordinate values encountered vertically from the NR/NB on the abscissa

for specific total cycle times of 1000, 2000 and 3000 seconds. For selections of trial parameters leading to acceptable designs, unique values of inlet velocities and bed length are found. For improperly selected sets of trial parameters no bed length and inlet velocity values will be found. The total cored ceramic brick mass required by the acceptable design conditions can be found by referring to the correct figure for total ceramic mass (Figures 18 - 20).

The temperature droop of the blowdown stream from the start to the end of the cycle is an important consideration in the design selection process. As shown for idealized conditions in Figure 2, the initial blowdown exit temperature is somewhat higher than the final. The magnitude of this temperature droop and the number of heat exchangers in operation, in theory, dictate the variation of the temperature of preheated air entering the MHD combustor. Temperature droop of the blowdown air exiting from the individual air preheaters, as calculated by the lumped mass model, are presented in Figures 21 and 22.

4.1.2 Sensitivity of Air Preheater Performance To Variation In Flow And Geometric Parameters

The lumped mass model was used to calculate changes in the average blowdown exit temperature and maximum thermal stresses using variations in flow and geometric properties. The variations were made from a single control base case. The control case used the inlet temperatures and flow conditions of ECAS Open Cycle MHD Base Case 1 [36] as

indicated in Section 4.1.1 and the following parameters

D = 38.1 mm

S/D = 1.40

L = 8 m

RTI + BTI = 1000 sec.

NR = NB = 5 (NR/NB = 1)

The average blowdown exit temperature ($TEXIT_{BD}$) and the maximum thermal stress (σ_{max}) were studied as functions of the inlet reheat velocity for each of the variations from the control case. Velocity dependent profiles of TEXIT and σ_{max} are shown in Figures 23 to 32 and discussed in Section 4.2.2 for simulations exhibiting variations from the control case of

1) D = 19.05, 25.4, 38.1, 44.5 and 50.8 mm (Figs. 23,24)
   and control case values of S/D, L, RTI+BTI, and NR/NB
2) L = 4,6,8,10,12 m (Figs. 25,26)
   and control case values of D, S/D, RTI+BTI and NR/NB
3) S/D = 1.20, 1.30, 1.40, 1.50 and 1.60 (Figs. 27,28)
   and control case values of D, L, RTI+BTI and NR/NB
4) RTI+BTI = 500, 1000, 2000 and 3000 sec. (Figs. 29,30)
   and control case values of D, S/D, L, and NR/NB
5) NR/NB = 3/6, 4/6, 5/5, 6/4 and 6/3 (Figs. 31,32)
   and control case values of D, S/D, L and RTI+BTI.

Figures 33 and 34 show TEXIT and σ_{max} as functions of inlet reheat velocity with control case values of D, L, S/D, RTI+BTI and NR/NB using several values for the inlet reheat gas temperature. Figures 35 and 36 show TEXIT and σ_{max} as functions of the bed length with control case values of D, S/D, RTI+BTI and NR/NB for several values of the inlet reheat velocity.

The sensitivity studies were carried out for greater ranges of the design parameters than those that led to acceptable MHD air preheater designs. Specifically for low S/D, low D, high total cycle time and high stress levels the blowdown exit temperature droop criteria was exceeded. The calculated results in this unacceptable design region are indicated by dashed lines.

These studies using the numerous variations in parameters and showing TEXIT and σ_{max} as functions of the reheat inlet gas velocity were completed to aid in the design of full scale air preheaters, specifically those presented in Section 4.1.1. Figures 23 to 36 were used in the design process to provide initial approximations for L and V1. The figures also gave an indication of the magnitudes of $\frac{\partial \sigma_{max}}{\partial V1}$, $\frac{\partial TEXIT}{\partial V1}$, $\frac{\partial \sigma_{max}}{\partial L}$ and $\frac{\partial TEXIT}{\partial L}$ at the approximated values of L and V1, which are an aid in determining the sensitivity of TEXIT and σ_{max} to changes in L and V1.

4.1.3 Designs for MTSFF

The lumped mass model was used to predict thermal characteristics for an experimental cored brick heat exchanger facility being utilized at Montana State University to examine slag deposition on the ceramic tube walls. The Moderate Temperature Slag Flow Facility (MTSFF) has a fixed geometry bed with characteristic dimensions of

$$L = 6.1 \text{ m}$$

$$D = 19.05 \text{ mm}$$

$$S/D = 1.42$$

For initial testing, a single stack of 19 hole hexagonal pattern cored brick comprises the core of the MTSFF. Hot gas for the reheat stream is provided by a natural gas fired combustor capable of delivering 0.057 kg/sec at 0.1034 MPa and 1927 K. An air stream inductively heated from ambient to 339 K and at flow rates up to 0.057 kg/sec at 0.1034 MPa provides a low pressure blowdown stream for the heat exchanger. The maximum operating conditions for the MTSFF are

Reheat gas inlet temperature	= 1927 K
Reheat gas inlet pressure	= 0.1034 MPa
Reheat gas mass flow rate	= 0.057 kg/sec
Blowdown air inlet temperature	= 339 K
Blowdown air inlet pressure	= 0.1034 MPa
Blowdown air mass flow rate	= 0.057 kg/sec

For the hole geometry and flow capacity of the MTSFF, the maximum reheat

inlet velocity is 56.0 mps at the temperature and pressure specified above. The maximum blowdown inlet velocity attainable is 9.86 mps. A maximum ceramic temperature limit of 811 K was imposed for the bottom of the MTSFF to insure the integrity of the metal structure supporting the ceramic core.

The lumped mass model was used to predict the cylical temperatures for the flow values and core configuration of the MTSFF as an aid in selecting experimental conditions for the MTSFF. Various combinations of flow conditions and cycle times were simulated with the lumped mass model. Plots of results from these simulations include variations in the average blowdown exit temperature, the maximum thermally induced stresses in the ceramic, the maximum ceramic temperature at the base of the bed, and the average and maximum exit temperatures of the reheat stream.

The effect of total cycle time (RTI+BTI) was investigated using maximum flow conditions and an array of total cycle times ranging from 600 to 1400 seconds. Equal cycle times were assumed (RTI=BTI). Results are presented in Figure 37. For total cycle times above 1123 seconds, the maximum ceramic temperature of the base surpasses the 811 K limit, while the average blowdown exit temperature remains fairly constant for different total cycle times.

The effect of inlet velocities (V1 and V2) on exit conditions was examined using a constant ratio of V1/V2 and constant cycle times

(RTI=BTI=300 sec). Simulations were made using inlet velocities ranging from 62% of maximum to maximum values. A constant V1/V2 ratio of 5.675 was used which is the ratio of maximum reheat to blowdown velocities in the MTSFF. These results are presented in Figure 38. In contrast to Figure 37, the maximum base ceramic temperature remains fairly constant and the average blowdown temperature increases.

A third area of MTSFF simulation used maximum flow conditions in one cycle and less than maximum flows in the other cycle. This was done for both reheat and blowdown streams. These results are shown in Figures 39 and 40 and include the variation of the average blowdown exit temperature, maximum thermal stresses, reheat gas exit temperatures and the maximum ceramic temperature at the base of the MTSFF. The simulations were made for three values of total cycle time, 600, 1000 and 1400 seconds. In contrast to Figures 37 and 38, reheat and blowdown cycle times are not equal, but are determined as those times which satisfy;

$$\frac{\dot{m}_{RH} \times RTI}{\dot{m}_{BD} \times BTI} = 1.0 \qquad (32)$$

From Figures 39 and 40 it is seen that where $\dot{m}_{BD}/\dot{m}_{RH} = 1$, where both $\dot{m}_{BD}$ and $\dot{m}_{RH}$ are at their maximum, a limit is reached for the average blowdown exit temperature, the maximum thermal stress and the maximum base ceramic temperature. In the following section a discussion of results is presented.

4.2 Discussion of Designs and Simulations

This first part of this section contains a discussion and explanation of the design cases presented for air preheaters designated to operate under ECAS Open Cycle MHD Base Case 1 specifications. Trends concerning the core sizes, bed lengths, and flow conditions necessary to meet Base Case 1 are developed and characteristics of the total mass requirements for air preheater systems are identified.

The second part discusses variations of the cyclic equilibrium conditions in an air preheater operation caused by modifications of the core geometry and flow rates. The discussion of these results includes an examination of the average blowdown exit temperature and the maximum thermally induced stresses in the ceramic. The effects of changes in flow hole diameter, bed length, inlet velocities, S/D ratio, NR/NB ratio, total cycle time and inlet gas temperature are also included. Results are presented in graphical form, generally as plots of the average blowdown exit temperature or maximum thermal stress as functions of the reheat inlet velocity for various values of geometric, time, or temperature variables.

Results of the Moderate Temperature Slag Flow Facility (MTSFF) computer simulations are also discussed.

4.2.1 ECAS Base Case 1

The cored ceramic brick air preheater system designs presented in section 4.1.1 and indexed in Table 1 represent heat exchangers with hole diameters of 19.95, 38.1 and 50.8 mm. and hole spacing to diameter ratios of 1.20, 1.40, and 1.60. Heat exchangers were designed using the lumped mass model to operate for total cycle times (RTI+BTI) of 1000, 2000 and 3000 seconds with a range of NR/NB ratios. Bed length and velocities were determined for each design which resulted in the blowdown exit temperature having an average value of 1644 K, a maximum thermal stress in the ceramic of either 13.79 or 34.47 MPa and a blowdown exit temperature droop of less than 100 K. The temperatures, pressures and flow rates simulated are those of a full scale MHD power-generating system; specifically, those designated in ECAS Open Cycle MHD Base Case 1.

Although each of the Base Case 1 air preheater system designs meet the temperature and thermal stress limits specified as design criteria, the cored brick mass requirements are different for each configuration. The selection of the most economical air preheater designs for incorporation in full scale MHD systems must include careful investigation of the total mass requirements of cored brick in the preheater beds. The total mass of the ceramic core is closely associated with the total costs of the air preheater system for open cycle MHD. An air preheater system with a smaller amount of cored brick will in most cases have a

lower cost than one requiring larger amounts of brick. The total cored brick mass of an air preheater system is calculated by multiplying the ceramic mass per heat exchanger by the total number of heat exchangers in operation, specifically, the number in reheat mode and blowdown mode at any time plus two heat exchangers designated to be in a switchover operation at any time.

General Ceramic Mass Requirements

The total ceramic mass requirements for the air preheater system are shown in Figures 18 to 20, and classified according to hole diameter and maximum thermal stress level in the ceramic. From these figures it is observed that minimum total ceramic mass for the designs investigated is found in a design utilizing the 50.8 mm. hole diameter, and S/D ratio of 1.20, a total cycle time of 1000 seconds, a maximum thermal stress level of 13.79 MPa and a NR/NB ratio of 4/6. The total ceramic mass required for this design case is 6.16×10^5 Kg. The maximum total mass requirement for any of the preheater systems calculated was 65×10^5 Kg or approximately 10 times the minimum value. The maximum was calculated for a design case using a hole diameter, D, of 50.8 mm, and S/D ratio of 1.60, total cycle time of 3000 seconds, maximum thermal stress of 13.79 MPa, and an NR/NB ratio of 6/3. The remainder of the design cases indicate ceramic requirements which are distributed fairly uniformly between the minimum and maximum values.

Heat exchanger design parameters of D, S/D, RTI+BTI, maximum thermal stress and NR/NB can each be associated with a trend in the total mass requirements. Stated in most general of terms; designs with high values of D, S/D, RTI+BTI or NR/NB require a larger total ceramic mass than do designs with low values of these parameters and designs with "low" thermal stress require more ceramic than designs with a "high" stress limit. Also it may be noted that as the ceramic mass requirement is reduced the blowdown exit temperature droop increases.

Effect of Diameter

Smaller ceramic masses result for small diameter designs mainly because the ratio of convective heat transfer area to ceramic volume is larger for small diameters. This ratio is

$$\frac{A_{conv}}{Vol_{cer}} = \frac{1}{D} \frac{1}{(S/D)^2 \cos(\pi/6) - .25} \qquad (33)$$

For a hole diameter, D, of .01905 m, and S/D = 1.60, equation (33) has a value of 26.69 m^{-1}. As the diameter increases to 38.1 mm., the convective area to volume ratio decreases to 13.34 m^{-1} and further decreases to 10.01 m^{-1} at D= 50.8 mm. For small diameters, there is less resistance to heat transfer per unit volume at the ceramic surface and heat can be exchanged more effectively between the gas and ceramic. This enables the ceramic mass surrounding each hole to be heated more rapidly during reheat. A secondary effect of the higher A_{conv}/Vol ratio

is a more uniform temperature across the ceramic. This uniformity of ceramic temperature leads to smaller thermal stresses. The flow rates of both streams can then be increased to higher values without exceeding thermal stress limits. Higher heat transfer coefficients associated with increased flow rates cause a reduction in the convective heat transfer area needed.

With larger hole diameters, the ratio of convective surface area to ceramic volume is reduced and greater resistance to heat transfer is encountered. The necessary heat transfer area is made up by increasing the length of the bed or by adding more tubes to each heat exchanger, both of which add mass.

For a given convective heat flux, the average ceramic temperature gradient is higher for geometries with larger hole sizes. The larger temperature gradient creates higher thermal stresses. A reduction in heat flux using lower velocities to meet stress limits is necessary, which increases ceramic mass. To achieve the essential total heat transfer, the bed must be lengthened and a larger area created for the lower heat flux. The reduced velocities and increases bed lengths for larger diameter holes are evident in the design cases and can be observed by examining Figures 9-17 for designs displaying variations only in the hole diameter. For example, Figures 9, 11, and 16 can be compared to show lower inlet velocities and longer bed lengths necessary as the hole diameter is increased.

S/D Effect

The ratio of convective surface area to ceramic volume is greater for smaller values of S/D. Using a constant diameter of 50.8 mm, the A_{conv}/Vol_{cer} ratio is 19.74 m^{-1} for S/D = 1.20, 13.60 m^{-1} for S/D = 1.40 and 10.00 m^{-1} for S/D = 1.60. With the larger A_{conv}/Vol_{cer} ratio associated with low S/D, the ceramic surrounding each hole can be heated more rapidly and a more uniform temperature across the ceramic can be maintained. Higher velocities are acceptable with lower S/D ratios while maintaining thermal stress levels which results in a lower flow area and a smaller ceramic mass.

The response time between a change in the surface temperature and changes in the average ceramic temperature also increases with S/D. Larger amounts of ceramic between holes create larger temperature differences between the average temperature and the surface temperature, and increase thermal stresses as S/D is increased for a given heat flux. To achieve the necessary heat transfer for a constant average blowdown temperature, it then becomes necessary to increase the bed length, which results in higher ceramic masses. The reduced velocities and longer bed lengths required when increasing the S/D ratio are evident in the design cases and can be observed by examining Figures 9-17 for designs displaying a variations only in the S/D ratio, for example, Figures 13, 14 and 16.

Effect of Total Cycle Time

For fixed geometry and ceramic properties, the thermal stresses at the inner wall of the ceramic tube vary linearly with Q, the heat flux between gas and ceramic, as is shown by equation (21). Setting a maximum limit for this stress in effect sets a maximum limit for the heat flux. The largest thermal stresses occur at the start of the cycle, when the largest temperature differences exist between gas and ceramic. Designs with long total cycle times exhibit fairly low heat flux levels at the end of reheat and blowdown periods. In comparing designs with variation only in total cycle time, initial heat flux values are fairly uniform. However, at the end of a cycle, designs with cycle times of 2000 seconds have only about half the heat flux as the 1000 second designs. The 3000 second designs have only about half the heat flux of the 2000 second designs at the end of blowdown cycles. The reduction in the heating rate for longer cycle times must be made up by lengthening the bed to provide more heat transfer area. The longer bed lengths necessary when increasing the total cycle time are evident in the design cases and can be observed by examining the variation in bed lengths for different total cycle times in each of Figures 9-17 for specific values of NR/NB.

Longer cycle times, specifically longer reheat times, raise the temperature profile of the ceramic at the end of reheat. The initial ceramic temperatures at the inlet end for reheat gases remain fairly

constant for the different cycle times, but as cycle times are increased the ceramic at the bottom of the heat exchangers has time to heat to higher temperatures. When the blowdown cycle begins and cool air enters the heat exchanger bottom, a larger gas to ceramic temperature difference exists there which raises the heat flux and the thermal stresses.

Exceptions to the trends of longer cycle times requiring longer bed lengths are noted in Figures 11 and 16 for NR/NB greater than 1.5. The reduced inlet velocities necessary for longer cycle times cause the reheat stream to fall into a laminar flow region. As NR/NB is increased, the 3000 second design undergoes a turbulent to laminar transition in the reheat stream at about NR/NB = 1.5 and the 2000 second design undergoes turbulent to laminar transition in the reheat stream at NR/NB between 1.5 and 2.0. At NR/NB = 2, the reheat stream of the 1000 second design is still not fully laminar, but is laminar in only the first 2/3 of the bed and turbulent thereafter. After a transition into laminar flow has occurred, the Nusselt number attains a constant value. More heat can be transferred between gas and ceramic per unit mass by reducing the flow rate rather than by increasing it, because of the longer residence time for a volume of gas traveling at lower rates. The lower velocities of the 3000 second designs and the length of the cycles combine to raise the temperature of the entire bed during reheat and permit more storage of energy per length of heat exchanger. Higher flow velocities for the 1000 second design raise the requirement for

energy transfer to turbulent blowdown stream. Because the reheat stream is still laminar, sufficient energy can only be transferred to the bed by increasing the bed length.

Effect of Stress Limit

Designs with maximum thermal stress limits of 34.47 MPa exhibit total ceramic mass requirements significantly lower than designs with thermal stress limits of 13.79 MPa. Larger heat flux values are acceptable which infers larger flow velocities and decreased bed length. These reductions in bed length and the higher flow velocities of the higher thermal stress designs combine to reduce total ceramic mass to 40 to 60% of that for low stress designs. Inlet velocities for the low stress designs are typically 55-65% of the inlet velocities for comparative high stress designs and bed lengths are typically 10% to 25% higher.

NR/NB Effect

As seen from Figures 18 to 20, the total ceramic mass requirements increase as the NR/NB ratio increases. To examine the primary reason for this, consider a fixed heat exchanger geometry. If the NR/NB ratio is increased from one value $(NR/NB)_1$ to a higher value $(NR/NB)_2$ the ratios of inlet velocities must be altered as seen from equation (A1.10). To determine the individual changes required in V1 and V2 as NR/NB is changed, equations (A1.10), (A1.11) and (A1.16) can be combined as

shown below.

$$\frac{NR_2\ V1_2}{(NR_2 + NB_2 + 2)} = \frac{NR_1\ V1_1}{(NR_1 + NB_1 + 2)} \tag{34}$$

and

$$\frac{NB_2\ V2_2}{(NR_2 + NB_2 + 2)} = \frac{NB_1\ V2_1}{(NR_1 + NB_1 + 2)} \tag{35}$$

or,

$$V1_2 = V1_1\ \frac{NR_1}{NR_2}\ \frac{NR_2 + NB_2 + 2}{NR_1 + NB_1 + 2} \tag{36}$$

$$V2_2 = V2_1\ \frac{NB_1}{NB_2}\ \frac{NR_2 + NB_2 + 2}{NR_1 + NB_1 + 2} \tag{37}$$

For example, when going from a system with NR/NB = 5/5 ($NR_1 = 5$, $NB_1 = 5$) to a system with NR/NB = 6/4 ($NR_2 = 6$, $NB_2 = 4$);

$$V2_2 = \frac{5}{4}\ V2_1$$

$$V1_2 = \frac{5}{6}\ V1_1$$

As the NR/NB ratios are increased, the value of V2 required for the fixed geometry increases. However, due to the maximum thermal stress limits imposed on the designs, higher blowdown velocities raise the heat flux in the system and cause excess thermal stresses. Therefore, V2 usually can not be raised as required while maintaining constant stress levels. Therefore, the geometry must be altered to accomodate the NR/NB change. The geometry change is usually in the direction of increasing ceramic mass.

To maintain a fixed stress level, the ceramic mass must be increased according to

$$M_2 = M_1 \frac{V2_2}{V2_1} \frac{NB_2}{NB_1} \frac{NR_1 + NB_1 + 2}{NR_2 + NB_2 + 2} \qquad (38)$$

where $V2_2$ is the maximum blowdown velocity as the thermal stress level is approached. This relation expresses the mass gain by altering the number of flow holes while assuming the bed length is held constant. Generally, bed lengths for high stress designs were fairly constant with NR/NB as can be seen in Figures 12, 15 and 17.

For low stress designs, the required bed lengths increase considerably with NR/NB. The increases in bed length further increase the ceramic mas requirements in addition to those defined by equation (38). The increases in bed length for high NR/NB in the low stress designs are due to decreases in V1 according to equation (36) which reduces the heat flux into the ceramic during reheat. The reduced heating of the bed is not sufficient to maintain the necessary average blowdown temperature so the heat storage volume must be increased by lengthening the bed.

For sufficiently low reheat velocities at high NR/NB, a transition from turbulent to laminar occurs in the reheat stream. The longer residence time of the reheat gas overcomes the effects of a constant Nusselt number and causes a decrease in the necessary bed length to transfer the required amount of heat. This transition was encountered

in some of the low stress designs and can be observed in Figures 9, 11 and 16.

Blowdown Temperature Droop

An important problem related to the low ceramic mass designs and associated with thermal characteristics of the air preheaters is the magnitude of the blowdown air discharge temperature droop over the duration of a blowdown cycle. The temperature droop is calculated as the difference between the initial blowdown exit temperature and the final blowdown exit temperature. Negligible droop is desired to maintain a constant preheat temperature, but this is impractical. The sequencing of the individual heat exchangers discussed in section 3.1.1 is used to reduce the preheat air temperature ripple to acceptable levels. The individual heat exchanger blowdown exit temperature droop tends to follow trends opposite those of the ceramic mass relations. Designs with small ceramic mass tend to have high blowdown temperature droops. The largest droops are associated with high stress designs using small diameter, small S/D ratio and small ratios of NR/NB. Many of the tentative designs in these ranges of parameters were eliminated on the maximum droop criterion.

The only exception to the low mass-high temperature droop argument occurs in designs with low total cycle times. Less ceramic mass is required for designs with shorter cycle times and these designs also

exhibit less temperature droop than designs with longer cycle times. One of the strongest factors effecting the blowdown exit temperature droop is the S/D ratio, which dictates the relative amount of ceramic surrounding each hole. Figures 21 and 22 display the blowdown temperature droop for the three S/D ratios used in the design cases as functions of the NR/NB ratio. Separate plots are presented for the low and high stress levels. The blowdown temperatures droop for up to three hole sizes and up to three cycle times are included on each plot. Maximum blowdown temperature droop is found in the S/D = 1.20, D = 50.8 mm, low stress design. This also corresponds to the minimum ceramic mass design. The S/D = 1.6, D = 50.8 mm, low stress design exhibited the lowest blowdown temperature droop. The droop decreases as NR/NB is increased as seen in Figures 21 and 22. This is due to the increased mass and lower blowdown cycle times of higher NR/NB designs.

Roughness Effects

The design cases listed in Table I were completed with the lumped mass model using a wall roughness of 0.254 mm. Other wall roughnesses were tested for their effect on the air preheater designs. Changes in wall roughness led to only minimal variation in the total mass requirements for the air-preheater systems. Comparative design calculations were made for a smooth tube (zero roughness) and a tube with a roughness

of 0.254 mm. The necessary changes in bed lengths and inlet velocities to maintain stress limits and the average blowdown temperature combined to produce designs with small changes in total ceramic mass. Designs with smooth walls required longer beds to make up for their reduced heat transfer rates. In addition they also permitted higher flow rates to attain allowable thermal stress values. Designs with rough walls had higher heat transfer rates so needed shorter bed lengths, but also required reductions in flow rates to decrease thermal stresses. The changes in bed lengths and velocities offset each other and resulted in small changes in total ceramic mass. Two sets of acceptable designs were developed using both the zero wall roughness and the 0.254 mm wall roughness. The results are tabulated in Table 2 and show small variations in mass. For the two cases shown, the total ceramic mass required by the smooth wall designs is about 2.9% less than that required by the 0.254 mm wall roughness designs. The same comparative calculations were carried out for several other designs which did not satisfy the maximum blowdown droop criterion. In each case the smooth wall design required from 0.67% to 2.9% less ceramic than the corresponding rough wall design.

It is evident that ceramic core mass requirements for air preheater systems can be reduced by reducing hole diameters, S/D ratios, total cycle times, NR/NB ratios and operating the heat exchanger as close as possible to the maximum thermal stresses limit in the ceramic.

Aside from the blowdown exit temperature droop problems, there are several reasons why it is either undesirable or impossible to operate at limiting values for these parameters. The primary drawbacks of reducing hole diameters in the air heaters include the increased susceptibility of plugging or restriction of flow by deposition of seed and slag on the tube walls and the increased costs and difficulties of brick manufacture. Brick manufacturing costs also tend to increase as the S/D ratio for the bricks is reduced. The thinner walls for low S/D tend to increase the chances for failure after stress cracks have been initiated. As shorter cycle times are used, an increased frequency of valving is necessary. As higher thermal stress levels are approached, the risk of brick failure also increases.

4.2.2 Sensitivity of Air Preheater Performance to Variations in Flow and Geometric Parameters

A series of heat exchanger configurations was studied using the lumped mass model to determine the effect of flow velocity on the average blowdown exit temperature (TEXIT) and maximum thermal stresses in the ceramic. Inlet temperatures and flow conditions for this series of air preheater simulations met the requirements of the General Electric ECAS Open Cycle MHD Base Case 1 [36]. Results are presented in graphical form in Figures 23 to 36. Variations of hole diameter, S/D ratio, bed length, NR/NB ratio, total cycle time (RTI+BTI) and inlet reheat temperature were made from a control case, and the velocity dependence of TEXIT and thermal stress were observed. The control case used in this section was a heat exchanger configuration with a hole diameter of 38.1 mm, S/D ratio of 1.40, NR/NB = 5/5, RTI = BTI = 1000 seconds, and bed length of 8 meters. The sensitivity calculations were extended beyond the ranges in parameters leading to acceptable designs in terms of blowdown exit temperature droop. These results are shown as dashed lines in the figures.

Control Case

A graph of blowdown exit temperatures as a function of the inlet reheat velocity for the control case is shown in Figure 8. For inlet reheat velocities less than 16 mps, both the reheat and blowdown

streams are in laminar flow. Above V1 = 16 mps, both streams enter turbulent flow. As velocities are increased, the increased heat flux into the ceramic causes the blowdown exit temperatures to rise. The increase of the blowdown exit temperatures continues until a maximum is reached at a velocity of about 45 mps. Above this velocity, the mass flow is increasing at a faster rate than the rate of heat transfer, causing less heat transfer per unit mass of blowdown air.

Effect of Diameter

The hole diameter was varied from the control case value. The results in Figure 23 show the average blowdown exit temperature (TEXIT) as a function of velocity for six values of hole diameter. The TEXIT - velocity patterns are similar for each of the hole diameters, but differ in both magnitude and location of the laminar-turbulent transition. Small diameter cases undergo transition at a lower velocity than large diameter cases due to the linear dependence of the Reynolds number on diameter. The magnitude of TEXIT is greater for the small diameter holes, due to the increased A_{conv}/Vol_{cer} ratio discussed at the beginning of section 4.2.1, which causes more effective heat transfer for the lower diameter holes. The thermal stress-velocity relation is shown in Figure 24. As expected, the largest stresses are associated with the large diameter holes.

Effect of Bed Length

The bed length was varied from the control case to find the effect of inlet velocity on TEXIT and maximum thermal stress at different bed lengths. These results are shown in Figures 25 and 26. The TEXIT-velocity patterns are all similar in shape but vary in magnitude. As expected, longer beds can store more energy to heat the blowdown air to higher temperatures. The shorter beds are heated to a higher average temperature during a reheat cycle causing larger thermal stresses when exposed to the cool blowdown stream as evidenced in Figure 26.

Effect of Total Cycle Time

As total cycle times are increased, the maximum value for TEXIT can be expected to decrease as shown in Figure 27. Heat transfer is reduced over the latter portion of a cycle as ceramic temperatures approach the gas or air temperatures. As expected, thermal stresses are higher for longer cycle times due to the increased heating of the bottom portions of the heat exchanger during reheat. The cool blowdown air makes contact with the higher temperature ceramic and produces increased thermal stresses. Figure 28 displays the increased stresses at higher total cycle times.

Effect of NR/NB

The TEXIT-velocity study was made using several ratios of NR/NB and the same core configuration as the control case. TEXIT-velocity

profiles for NR/NB ratios of 3/6, 4/6, 6/4 and 6/3 were made in addition to the control case which used a NR/NB ratio of 5/5. In contrast to the control case where transition from laminar to turbulent took place at the same inlet reheat velocity for both blowdown and reheat streams, two instances of laminar to turbulent transition were noted for cases using other values of NR/NB as shown in Figure 29. For cases where NR/NB was greater than 1.0, the blowdown stream went under laminar to turbulent transition before the reheat stream as V1 was increased. This first transition is evident in Figure 29 at an NR/NB ratio of 6/3. The blowdown stream for this case became turbulent when the reheat velocity became 9 mps and caused the small rise in TEXIT between 9 and 12.5 mps. Raising the inlet velocity while the reheat stream remained laminar caused less total energy per unit mass of reheat gas to enter the bed during reheat and caused TEXIT to drop. At V1 = 16 mps, the reheat stream became turbulent and TEXIT began to rise until a maximum was reached where increases in mass flow rate overcame increases in heat transfer. The dual transition also existed for NR/NB = 6/4 but occurred over too small a velocity interval to cause an observable inflection in TEXIT.

For values of NR/NB less than 1.0, the reheat stream became turbulent prior to the blowdown stream causing a temporary increase in TEXIT before increases in the flow rate lowered TEXIT. The second transition (blowdown stream laminar to turbulent) again caused TEXIT to

increase.

Figure 30 shows the thermal stress velocity relation for various values of NR/NB. As expected, thermal stresses are highest for cases having NR/NB = 6/3. For a given reheat velocity, the blowdown velocities are highest at high NR/NB as shown by equation (A1.10) in Appendix I causing higher thermal stresses.

Effect of S/D

Figures 31 and 32 show the TEXIT-velocity relations and the thermal stress-velocity relations for various ratios of S/D. Little variation in values of maximum TEXIT exist between cases using S/D ratios of 1.40, 1.50 and 1.60. The maximum values for TEXIT decrease as S/D is reduced to 1.30 and 1.20 due to the reduction in heat storage medium surrounding the flow holes for lower S/D.

As expected, thermal stresses increase with both velocity and S/D as shown in Figure 32. There are greater temperature gradients in the ceramic for the S/D = 1.60 cases causing larger thermal stress values.

Effect of Inlet Reheat Gas Temperatures

An anticipated result of increasing the reheat gas inlet temperature is an increase in the blowdown exit temperature. Figure 33 displays the variation in TEXIT for variations in the reheat inlet temperature. Equal steps in the inlet reheat temperature resulted in equal steps in TEXIT. Gases with higher inlet reheat temperature

exhibited higher thermal stress values because of the increased ceramic-to-gas temperatures differences in blowdown as shown in Figure 34.

Effect of Bed Length

A slightly different format is used in Figures 35 and 36 which show TEXIT and maximum thermal stresses as functions of the bed length for various values of the inlet reheat velocity. Maximum values for TEXIT for any bed length are found between inlet reheat velocities of 40 and 50 mps. At lower velocities, heat transfer rates drop off reducing TEXIT while at higher velocities, the mass flow rate is increasing faster than the heating rates increase, resulting in a lower TEXIT.

As expected higher thermal stress levels are found when using higher velocities and/or shorter bed lengths as shown in Figure 36.

Many such comparisons can be made as those displayed in Figures 23 to 36 which show reheat temperatures, pressure drops as well as TEXIT and thermal stresses as functions of variations in such parameters as inlet reheat pressure, inlet blowdown temperature or pressure, reheat or blowdown mass flow rates or tube roughnesses. More importance was placed on those variables which were chosen (L, S/D, NR/NB, RTI+BTI, V1, TEXIT and thermal stress) because these dictate the effectiveness of a heat exchanger and control the sizes and costs. Figures 23-36 were used as an aid in completing the Base Case 1 air preheater designs for which TEXIT and the maximum thermal stress formed important design

criteria. The Newton-Raphson method for selecting bed lengths and inlet velocities (section 3.32) relied upon finding variation of both stress and TEXIT with inlet velocity which Figures 23 to 32 show for a multitude of conditions. Variations in thermal stress and TEXIT with bed length were used in the Newton-Raphson method and Figures 35 and 36 show these variations for a typical case.

The relations shown in Figure 23 to 36 can also be used as tools in designing regenerative cored brick heat exchangers. Although the conditions used in the formation of these figures are not all-encompassing, they show basic trends produced by variations in major design parameters.

4.2.3 MTSFF Designs

The Moderate Temperature Slag Flow Facility (MTSFF) being constructed at Montana State University is a small scale cored ceramic brick regenerative heat exchanger and will be used to experimentally determine the characteristics of coal slag deposition. Various bed configurations are designated for study, however the initial core is composed of a single T9 hole hexagonal brick with 19.05 mm. diameter holes in a hexagonal array and an S/D ratio of 1.42. The brick material for the initial MTSFF core is Corhart RFG, a rebonded fused grain magnesia-chromite material. Material properties for RFG were used in all lumped mass model calculations.

The lumped mass model code was used to predict cyclic equilibrium thermal-hydraulic operational characteristics for the MTSFF. The MTSFF operation was simulated with the lumped mass model using anticipated operating conditions as trial design criteria. These conditions were given in section 4.1.3.

Effect of Total Cycle Time

The effect of total cycle time for the MTSFF was investigated using conditions of maximum flow for both reheat and blowdown. Reheat and blowdown time were assumed equal and their total was varied from 600 to 1400 seconds. Figure 37 shows the exit reheat and blowdown temperatures, the maximum thermal stresses and the maximum base ceramic

temperature of the heat exchanger as functions of the total cycle time. The average reheat and blowdown exit temperatures are almost constant over the range of total cycle times while the maximum ceramic temperature at the base and the maximum thermal stress are increasing at approximately constant rates. Increased amounts of energy being transferred to the heat exchanger over the longer cycles enable the lower sections of the heat exchanger to be heated to higher temperatures. When blowdown is started, the warmer bottom end is subjected to a cold blowdown stream causing the maximum thermal stresses to increase at a rate similar to the rate of increase of the base ceramic temperature.

Flow Rate Effect

A second area for simulation of the MTSFF investigated cases where both reheat and blowdown flow rates were less than maximum. Reheat and blowdown cycles each had a duration of 300 seconds and mass flow rates of both streams were equal. The effect of decreasing flow rates from their maximum to about two-thirds of maximum was studied and results are shown in Figure 38. As expected, the rate of heat transfer increases as flow rates approach maximum values causing the average blowdown exit temperature and thermal stresses to increase. Reheat exit temperatures decrease as the reheat stream gives up greater amounts of its energy to the ceramic at high flow rates. The maximum ceramic temperature at the base maintains a fairly constant value which is

expected for the short reheat time used.

The third area for simulation of the MTSFF was for cases where the reheat mass flow rate was at its maximum and the blowdown flow rate varied from 70 to 100 percent of maximum and cases where the blowdown flow rate was at its maximum and the reheat flow rate was varied from 50 to 100 percent of maximum. Three values for total cycle time were used. The reheat and blowdown cycle times were not equal but were varied according to the relationship

$$\frac{\dot{m}_{RH} \times RTI}{\dot{m}_{BD} \times BTI} = 1 \qquad (32)$$

Temperatures and thermal stresses for these simulations using variable ratios of mass flow are shown in Figures 39 and 40 as functions of $\dot{m}_{BD}/\dot{m}_{RH}$. Maximum values for average blowdown exit temperature, thermal stress and base ceramic temperature occur at $\dot{m}_{BD}/\dot{m}_{RH} = 1$. The reheat exit gas temperatures have a minimum at this point because at $\dot{m}_{BD}/\dot{m}_{RH}$, the heat transfer rates for each cycle are highest.

Thermal stresses again increase with total cycle time as does the maximum ceramic temperature of the base. The maximum ceramic temperature at the base of the MTSFF heat exchanger is fairly important criteria. The bed is supported by a metal structure having a limited maximum temperature for which it retains structural integrity. This temperature limit for the MTSFF designs was set at 811 K and serves as

an important consideration in selecting experimental operating conditions for the MTSFF facility. The ceramic temperature limit is exceeded at a total time of about 1125 seconds with designs made with maximum flow rates for both reheat and blowdown streams. This point can be located in Figure 40 at $\dot{m}_{BD}/\dot{m}_{RH} = 1$ by interpolating between lines of RTI+BTI = 1000 and RTI+BTI = 1400 seconds. For ratios of $\dot{m}_{BD}/\dot{m}_{RH}$ other than one, longer total cycle times can be utilized without surpassing the maximum MTSFF base ceramic temperature limit.

For the cases investigated it appears that the most effective operation of the MTSFF will be found using the maximum flow rates where RTI = BTI and RTI + BTI is less than 1125 seconds.

Chapter V

CONCLUSIONS

1) ECAS Base Case 1 conditions can be attained for a variety of cored ceramic brick heat exchanger designs.
2) Minimum cost or minimum ceramic mass designs result for lower D, lower S/D, lower total cycle time, lower NR/NB ratio, or higher thermal stress limits.
3) Changes in Item 2 parameters to reduce mass are severely limited by the maximum blowdown exit temperature droop criterion. Low ceramic mass designs are associated with high blowdown droop.
4) Changes in Item 2 parameters to reduce mass are also limited by potential plugging of smaller diameter holes, manufacturing difficulties for small diameter, small S/D ceramic bricks, increased valve operation frequency at lower cycle times, or failure of bricks at high termal stress levels.
5) Variations in tube roughness do little to affect the total ceramic mass, but instead alter the length and diameter of the bed while maintaining a nearly constant total mass value.
6) Design information and thermal-hydraulic operational trends have been established for multiple unit MHD air preheater systems.
7) The sensitivity of thermal equilibrium design characteristics to variations in flow and geometric properties has been established.

8) Simulations of the MTSFF cored brick heat exchanger were produced as aids for initial experimental operations.

TABLE 1

Parameter Variations Used in ECAS Open Cycle MHD Base Case 1 [36] Air Preheater Design Cases (Figures 9 - 17)

Figure	Hole Diameter (mm)	S/D Ratio	Stress Limit ($Pa \cdot 10^6$)	NR/NB Ratio Range	Total Cycle Time (seconds)	Figure Showing Total Ceramic Mass
9	19.05	1.6	13.79	4/6 - 6/3	1000,2000	18
10	38.10	1.4	13.79	" "	1000,2000,3000	18
11	"	1.6	13.79	" "	" " "	18
12	"	"	34.47	" "	1000,2000	18
13	50.80	1.20	13.79	" "	1000	19
14	"	1.4	13.79	3/7 - 6/3	1000,2000,3000	19
15	"	"	34.47	3/6 - 6/3	1000,2000	20
16	"	1.6	13.79	4/6 - 6/3	1000,2000,3000	19
17	"	"	34.47	" "	" " "	20

TABLE 2

Comparison of Inlet Velocities, Bed Lengths and Ceramic Requirements for Selected Thermal Design Cases Using Different Values of Wall Roughness

D (mm)	S/D	$\frac{NR}{NB}$	σ_{max} Limit	RTI +BTI (sec)	Wall Roughness (mm)	V1 (mps)	V2 (mps)	L (m)	Ceramic Mass kg · 10^4 per h.x.	Ceramic Mass kg · 10^4 Total
50.8	1.2	4/6	low	1000	0.0	45.00	1.68	6.92	4.99	59.87
					0.254	41.01	1.53	6.49	5.14	61.64
38.1	1.4	5/5	low	2000	0.0	27.13	1.51	6.41	1.21	14.53
					0.254	24.72	1.38	6.01	1.24	14.95

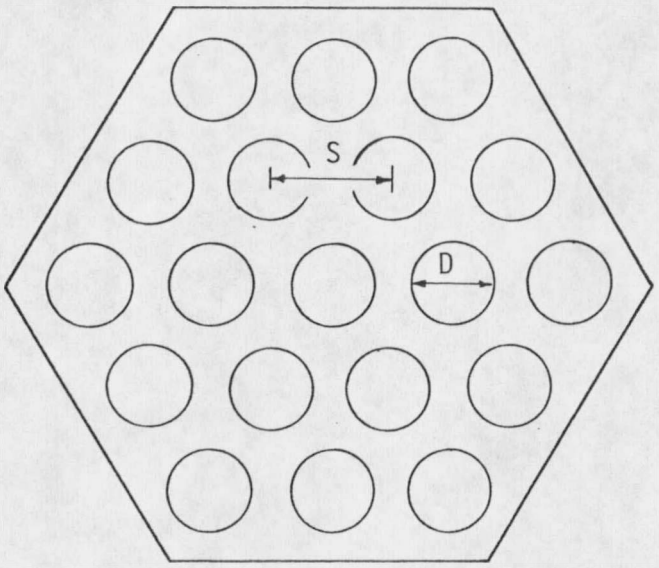

Hexagonal Cored Ceramic
Brick Configuration
Fig. 1 a

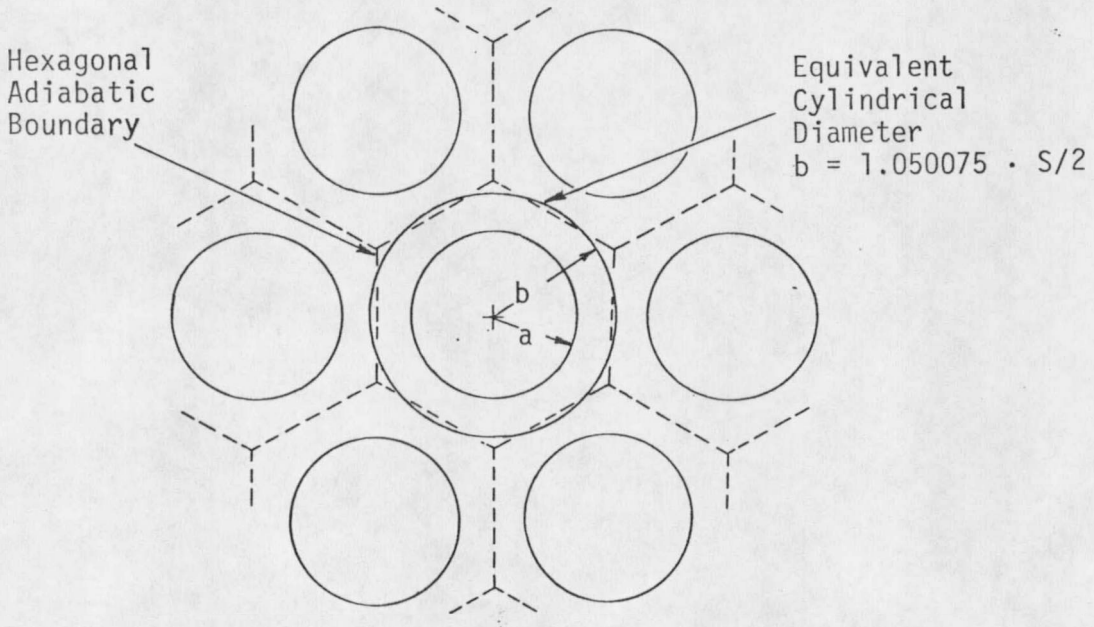

Location of
Adiabatic Surfaces
Fig. 1 b

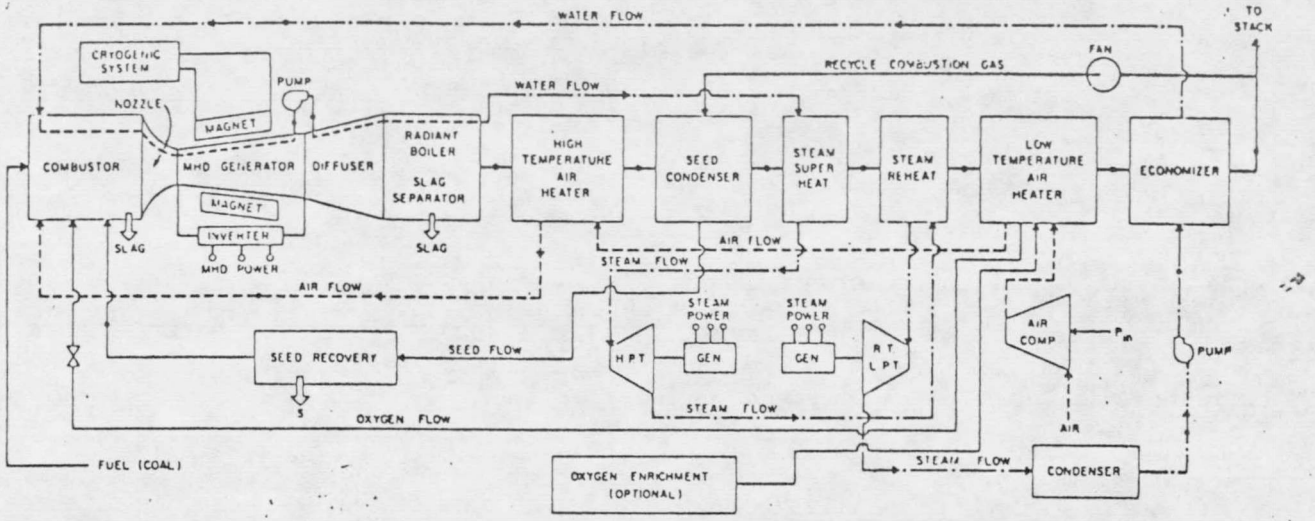

Fig. 2a MHD Schematic - Coal Fired/Directly Fired Air Preheater

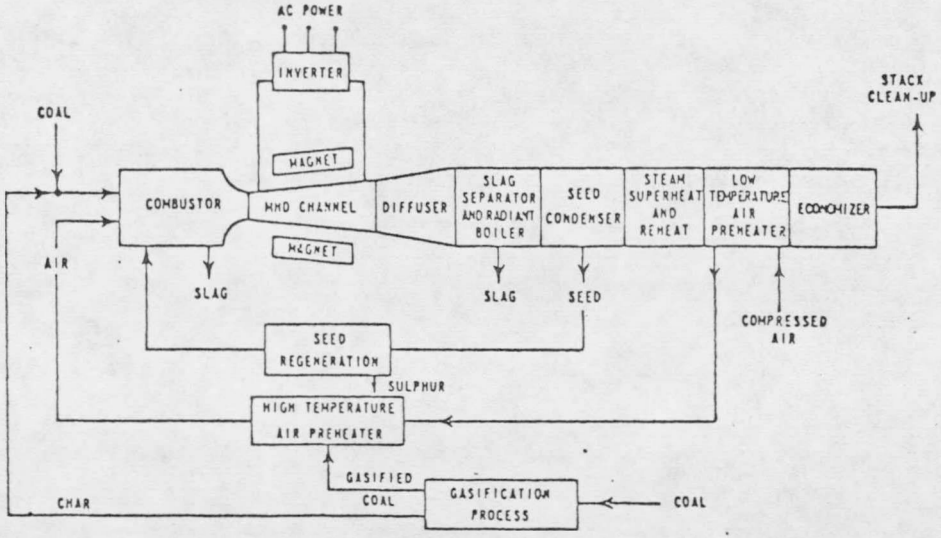

Fig. 2b MHD Schematic - Coal Fired/Indirectly Fired Air Preheater

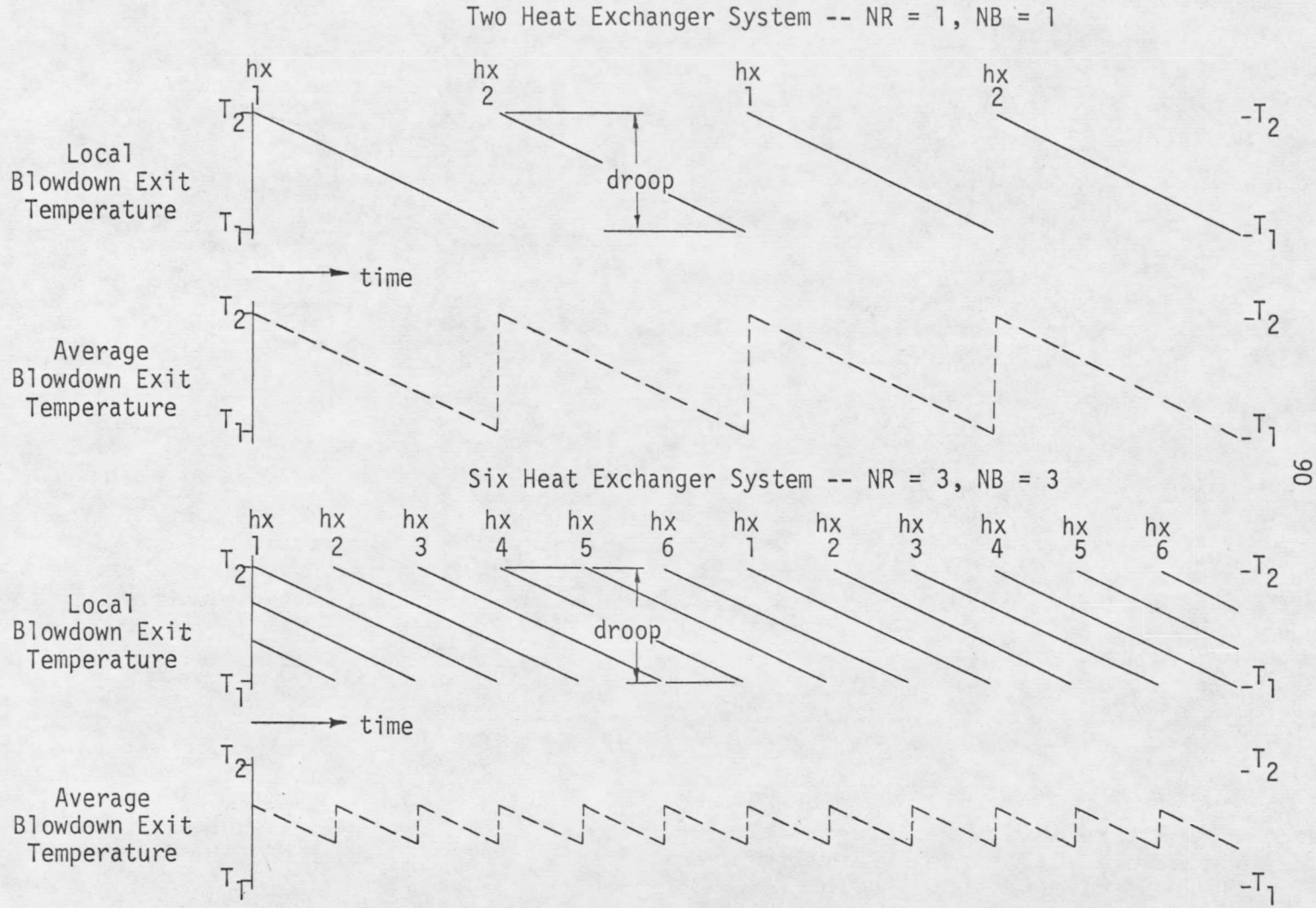

Fig. 3 Effect of Number of Heat Exchangers on Average Blowdown Temperature